

Resonant particle production with non-minimally coupled scalar fields in preheating after inflation

Shinji Tsujikawa^{1*}, Kei-ichi Maeda^{1,2†}, and Takashi Torii^{3‡}

¹ *Department of Physics, Waseda University, Shinjuku, Tokyo 169-8555, Japan*

² *Advanced Research Institute for Science and Engineering,
Waseda University, Shinjuku, Tokyo 169-8555, Japan*

³ *Department of Physics, Tokyo Institute of Technology, Meguro, Tokyo 152, Japan*

(October 22, 2018)

We investigate a resonant particle production of a scalar field χ coupled non-minimally to a spacetime curvature R ($\xi R\chi^2$) as well as to an inflaton field ϕ ($g^2\phi^2\chi^2$). In the case of $g \lesssim 3 \times 10^{-4}$, ξ effect assists g -resonance in certain parameter regimes. However, for $g \gtrsim 3 \times 10^{-4}$, g -resonance is not enhanced by ξ effect because of ξ suppression effect as well as a back reaction effect. If $\xi \approx -4$, the maximal fluctuation of produced χ -particle is $\sqrt{\langle \chi^2 \rangle}_{max} \approx 2 \times 10^{17}$ GeV for $g \lesssim 1 \times 10^{-5}$, which is larger than the minimally coupled case with $g \approx 1 \times 10^{-3}$.

98.80.Cq, 05.70.Fh, 11.15.Kc

I. INTRODUCTION

In an inflationary scenario, most of the elementary particles in the Universe were created during the stage of reheating after inflation [1]. During the inflationary stage, an inflaton field slowly rolls down to a minimum of its potential. A reheating process turns on when the inflaton field begins to oscillate around the minimum of its potential. The original version of reheating scenario was first considered in the context of a new inflationary model in [2,3]. The particles are created through an interaction term between the inflaton and some fields. A phenomenological decay term to describe the fact that the inflaton field decays to other lighter particles (radiation) is included in the equation of the inflaton field ϕ , and the energy of the inflaton is transferred to their thermal energy. According to this scenario, reheating temperature is determined by the decay rate Γ but not the initial value of ϕ . The value of Γ is constrained to be small by the perturbation theory such as $\Gamma < 10^{-20} M_{\text{PL}}$, where M_{PL} is the Planck mass, so the reheating temperature is estimated as $T_r < 10^9$ GeV. This temperature is not sufficient in order to produce baryon asymmetry based on Grand Unified Theories (GUTs).

Recently, however, it has been recognized that reheating process begins by a parametric amplification of scalar par-

*electronic address: shinji@gravity.phys.waseda.ac.jp

†electronic address: maeda@gravity.phys.waseda.ac.jp

‡electronic address: torii@th.phys.titech.ac.jp

ticles [4–7]. This initial evolutionary phase, which is called *preheating* stage, provides an explosive particle production and must be discussed separately from the perturbative decay of inflaton. There are many works about the preheating stage based on analytical investigations [8–11] as well as on numerical studies [12–14]. The important feature with the existence of preheating stage is that the maximal value of produced fluctuation can be so large that it would result in a non-thermal phase transition [15] and make baryogenesis at the GUT scale possible [16], although the baryogenesis might be important in much lower energy scale, i.e. the electro-weak scale [17].

So far, we know two possible preheating scenarios: one is that the inflaton field ϕ itself is transformed into many ϕ -particles from a coherent inflationary phase through a self-interaction such as $\lambda\phi^4$, and the other is that another field, e.g. a scalar field χ is created through some coupling with the inflaton such as $g^2\phi^2\chi^2$. Both cases were first discussed in [5] using Hartree mean-field approximation. For the former case, the preheating was studied [6,22] by making use of closed time path formalism [18–21], since the preheating is an essentially non-equilibrium state. They analyzed the non-perturbative evolution of the inflaton fluctuations for the self-interacting massive inflaton by the method of the $O(N)$ -vector model in the large N limit as well as by the Hartree factorization model, both of which are mean-field approximations. The $O(N)$ -vector model has an advantage to deal with the continuous symmetry while the Hartree factorization model is suitable to treat the discrete symmetry. To confirm the mean-field approximation, the fully non-linear numerical simulation including the scattering effect of created particles was also performed in [12] for the simple $\lambda\phi^4$ model, finding that the variance $\langle\delta\phi^2\rangle\sim 10^{-7}M_{\text{PL}}^2$ can be produced by the non-perturbative process of inflaton decay. They treated the scalar field fluctuations as classical ones, which would be justified because the fluctuations with rather low momenta are mainly produced by the parametric resonance. They found almost the same result as that by the mean-field approximation.

As for the case only with a massive-inflaton potential ($\frac{1}{2}m^2\phi^2$), the production of inflaton fluctuation will not be expected by a parametric resonance. Hence one usually introduces another scalar field χ coupled to the inflaton field ϕ through an interaction such as $g^2\phi^2\chi^2$. For the production of ϕ -particles in self-interacting case, the coupling is constrained to be $\lambda\sim 10^{-12}$ from the observation of COBE, while the coupling constant g in the present case is a free parameter. Hence we may find a higher production of χ -particles depending on the value of g . As for analytical investigation of χ -field evolution, Kofman, Linde and Starobinsky [5,8] developed the consistent theory of preheating based on Mathieu equation for χ -field. There are several numerical works devoted to the evolution of χ -field by fully non-linear simulations [13,14]. A parametric resonance turns on from the broad resonance regime in certain values

of the coupling g . The structure of resonance will be modified a lot in the expanding Universe compared with that in Minkowski space. The amplitude of the coherent ϕ field decreases adiabatically because of the expansion of the Universe, and eventually the resonance terminates. In the case that the coupling g is small and the resonance band is narrow from the first stage of preheating, an efficient resonance will not be expected. For the large coupling constant, the resonance band is broad in the beginning, and then we find a considerable production of χ -particles. In this case, χ -field crosses many instability and stability bands even within one oscillation of the inflaton field, and stochastic resonance occurs. A significant amplification occurs in the broad resonance regime, but in certain values of coupling constant g , production via such a resonance will be suppressed by a back reaction of created particles. When such a back reaction is taken into account, a coherent oscillation of the inflaton field is broken due to the increase of the effective mass of inflaton, and the energy of χ -field can not exceed much larger than that of ϕ -field at the final stage of preheating. Moreover, rescattering effect, which will also restrict χ -particles production, becomes important at the final stage of preheating.

Recently, another interesting mechanism for preheating called a geometric reheating model has been proposed by Bassett and Liberati [23]. They investigated the case that χ field is non-minimally coupled to spacetime curvature R for massive inflaton model and found that an explosive amplification of χ will be possible if the coupling constant ξ is negative [24]. This is just because of unstable modes with a negative coupling [25]. In this sense, it is different from ordinary parametric resonance. In particular, they studied how the homogeneous χ field is amplified and found that GUT scale gauge boson with mass $m_G \sim 10^{16}$ GeV can be produced in preheating stage when ξ is large negative.

A natural question may arise: If we combine both effects of g -resonance and ξ -resonance, whether we find more effective production of χ -particles, since small coupling g does not provide a sufficient production. It is of interest how the g -resonance picture is modified by taking into account the effect of geometric reheating. If the assisting mechanism works and final abundance of χ becomes rather larger, it may change the ordinary preheating picture and affect the non-thermal phase transition and baryogenesis. We will discuss such a combined resonance in detail. We also study the evolution of χ field fluctuation summed by all possible momentum modes in detail including the back reaction effect, because the previous study is mainly devoted to the growth of zero momentum mode at the initial stage of preheating [23].

This paper is organized as follows. In the next section, we introduce basic equations in the non-minimal preheating that includes ordinary g -resonance. The results of $g = 0, \xi > 0$ case is presented in Sec. III. We study the analytical

estimation as well as numerical results, and compare them with each other. In Sec. IV, we analyze $g = 0, \xi < 0$ case. The structure of negative coupling instability is investigated. In Sec. V, the combined effect of g and ξ resonance is studied. We present that at which values of g and ξ parametric resonance becomes most efficient. Finally, we give our discussions and conclusions in the final section.

II. BASIC EQUATIONS

We consider a model that an inflaton field ϕ is interacting with a scalar field χ , which is non-minimally coupled with the spacetime curvature R ,

$$\mathcal{L} = \sqrt{-g} \left[\frac{1}{2\kappa^2} R - \frac{1}{2} (\nabla\phi)^2 - V(\phi) - \frac{1}{2} (\nabla\chi)^2 - \frac{1}{2} m_\chi^2 \chi^2 - \frac{1}{2} g^2 \phi^2 \chi^2 - \frac{1}{2} \xi R \chi^2 \right], \quad (2.1)$$

where $\kappa^2/8\pi \equiv G = M_{\text{PL}}^{-2}$ is Newton's gravitational constant, g and ξ are coupling constants, and m_χ is a mass of the χ field. $V(\phi)$ is a potential of the inflaton field. In this paper we adopt the quadratic potential

$$V(\phi) = \frac{1}{2} m^2 \phi^2, \quad (2.2)$$

where m is a mass of the inflaton field, and we use the value of $m = 10^{-6} M_{\text{PL}}$ that is obtained by fitting density perturbations to COBE data.

Since non-minimal coupling between the spacetime curvature R and χ field makes the basic equations complicated, it is convenient to transform action (2.1) into the Einstein frame by a conformal transformation [26]. We make the conformal transformation as follows:

$$\hat{g}_{\mu\nu} = \Omega^2 g_{\mu\nu}, \quad (2.3)$$

where $\Omega^2 \equiv 1 - \xi \kappa^2 \chi^2$. The Lagrangian density in the Einstein frame becomes

$$\mathcal{L} = \sqrt{-\hat{g}} \left[\frac{1}{2\kappa^2} \hat{R} - \frac{1}{2\Omega^2} (\hat{\nabla}\phi)^2 - \frac{1}{2\Omega^4} m^2 \phi^2 - \frac{1}{2} F^2 (\hat{\nabla}\chi)^2 - \frac{1}{2\Omega^4} (m_\chi^2 + g^2 \phi^2) \chi^2 \right], \quad (2.4)$$

where variables with a caret denote those in the Einstein frame, and

$$F^2 = \frac{1 - (1 - 6\xi)\xi\kappa^2\chi^2}{(1 - \xi\kappa^2\chi^2)^2}. \quad (2.5)$$

To make the kinetic term of the χ field canonical, we define a new scalar field X as

$$X \equiv \int F(\chi) d\chi, \quad (2.6)$$

by which the Lagrangian density is now

$$\mathcal{L} = \sqrt{-\hat{g}} \left[\frac{1}{2\kappa^2} \hat{R} - \frac{1}{2\Omega^2} (\hat{\nabla}\phi)^2 - \frac{1}{2\Omega^4} m^2 \phi^2 - \frac{1}{2} (\hat{\nabla}X)^2 - \frac{1}{2\Omega^4} (m_\chi^2 + g^2 \phi^2) \chi^2(X) \right]. \quad (2.7)$$

Since we are interested in a preheating after inflation, as usual, we shall assume that the spacetime and the inflaton ϕ give a classical background and the scalar field χ is treated as a quantum field on that background. In the present model, however, there is some problem. We have performed a conformal transformation, which conformal factor Ω^2 includes quantum variable χ^2 . Then, in order not to discuss quantum gravity, the conformal factor should be replaced with some expectation value. Here, we regard the conformal factor Ω^2 as $1 - \eta$ [27], where

$$\eta \equiv \xi \kappa^2 \langle \chi^2 \rangle. \quad (2.8)$$

$\langle \chi^2 \rangle$ corresponds to the number density of the created χ -particle, where $\langle \dots \rangle$ denotes an expectation value of some functional of χ (or X).

With such a transformation, we assume that the spacetime and the inflaton field ϕ are spatially homogeneous, and adopt the flat Friedmann-Robertson-Walker metric as the background spacetime;

$$ds^2 = -dt^2 + \hat{a}^2(t) d\mathbf{x}^2. \quad (2.9)$$

Hereafter, as we argue only in the Einstein frame, we drop a caret. The evolution of the scale factor a yields

$$\left(\frac{\dot{a}}{a} \right)^2 = \frac{\kappa^2}{3} \left[\frac{1}{2(1-\eta)} \dot{\phi}^2 + \frac{1}{2(1-\eta)^2} m^2 \phi^2 + \frac{1}{2} \langle (\nabla X)^2 \rangle + \frac{1}{2(1-\eta)^2} (m_\chi^2 + g^2 \phi^2) \langle \chi^2 \rangle \right], \quad (2.10)$$

where a dot denotes a derivative with respect to time coordinate t .

The evolution of the inflaton field ϕ is described by

$$\ddot{\phi} + \left(3 \frac{\dot{a}}{a} + \frac{\dot{\eta}}{1-\eta} \right) \dot{\phi} + \frac{1}{1-\eta} (m^2 + g^2 \langle \chi^2 \rangle) \phi = 0. \quad (2.11)$$

Note that the fluctuation of the inflaton field $\delta\phi$ is not considered since we assume that the inflaton field is spatially homogeneous. However, the growth of the ϕ fluctuation would be expected to appear as χ field is amplified. Our investigations are limited in the sense that rescattering between χ and $\delta\phi$ fluctuation is not included.

In Eq. (2.11), if we introduce a new scalar field φ such as

$$\varphi \equiv b^{3/2} \phi, \quad (2.12)$$

where $b^3 = a^3/(1-\eta)$, then the field φ obeys the following equation:

$$\ddot{\varphi} + \left[\frac{1}{1-\eta} (m^2 + g^2 \langle \chi^2 \rangle) - \frac{3}{4} \left(\frac{2\ddot{b}}{b} + \frac{\dot{b}^2}{b^2} \right) \right] \varphi = 0. \quad (2.13)$$

Note that in the case of minimal coupling $\xi = 0$, η vanishes, hence the coherent oscillation of φ is broken only by $g^2 \langle \chi^2 \rangle$ term. As $\langle \chi^2 \rangle$ grows, the effective mass of the inflaton $m_{eff}^2 = m^2 + g^2 \langle \chi^2 \rangle$ gets large, i.e., oscillation becomes rapid. This effect, which is called back reaction effect to the inflaton field, suppresses the resonant particle creation. On the contrary, when ξ effect is taken into account, $1 - \eta$ is decreasing as $\langle \chi^2 \rangle$ grows, hence one may expect this effect also changes the coherent oscillation of φ . However, as we will see later, this is not the case and we can neglect ξ effect on the inflaton field in most cases.

Next, let us consider the equation of X field. The Heisenberg equation of motion is derived from (2.7):

$$\ddot{X} + 3\frac{\dot{a}}{a}\dot{X} - \partial_i \partial^i X - \frac{\partial}{\partial X} \left[\frac{\dot{\phi}^2}{2\Omega^2} - \frac{1}{2\Omega^4} m^2 \phi^2 - \frac{1}{2\Omega^4} (m_\chi^2 + g^2 \phi^2) \chi^2 \right] = 0, \quad (2.14)$$

where an index with a roman character denotes space coordinates. In order to study a quantum particle creation of χ fields, we make the following mean field approximation with respect to X , which provides us a linearized equation for a quantum field X :

$$\ddot{X} + 3\frac{\dot{a}}{a}\dot{X} - \partial_i \partial^i X - \nabla_X^2 \left[\frac{\dot{\phi}^2}{2\Omega^2} - \frac{1}{2\Omega^4} m^2 \phi^2 - \frac{1}{2\Omega^4} (m_\chi^2 + g^2 \phi^2) \langle \chi^2 \rangle \right] X = 0, \quad (2.15)$$

where $\nabla_X = 2\sqrt{\langle X^2 \rangle} \partial / \partial \langle X^2 \rangle$. From the relation (2.6), we have also assumed

$$d\left(\sqrt{\langle X^2 \rangle}\right) = \sqrt{\langle F^2 \rangle} d\left(\sqrt{\langle \chi^2 \rangle}\right), \quad (2.16)$$

where $\langle F^2 \rangle = [1 - (1 - 6\xi)\eta] / (1 - \eta)^2$. Expanding the scalar fields X as

$$X = \frac{1}{(2\pi)^{3/2}} \int \left(a_k X_k(t) e^{-i\mathbf{k}\cdot\mathbf{x}} + a_k^\dagger X_k^*(t) e^{i\mathbf{k}\cdot\mathbf{x}} \right) d^3\mathbf{k}, \quad (2.17)$$

where a_k and a_k^\dagger are the annihilation and creation operators, we find that X_k obeys the following equation of motion:

$$\ddot{X}_k + 3\frac{\dot{a}}{a}\dot{X}_k + \left[\frac{k^2}{a^2} + G(\langle \chi^2 \rangle) \right] X_k = 0, \quad (2.18)$$

with

$$G(\langle \chi^2 \rangle) \equiv \frac{1}{(1-\eta)[1-(1-6\xi)\eta]} \left[(1+3\eta)(m_\chi^2 + g^2 \phi^2) + 2\xi\kappa^2 m^2 \phi^2 - (1-3\eta)\xi\kappa^2 \dot{\phi}^2 \right] + \frac{\eta}{1-\eta} \frac{4 + (1-5\eta)(1-6\xi)}{1-(1-6\xi)\eta} \left\{ (1+\eta)(m_\chi^2 + g^2 \phi^2) + 2\xi\kappa^2 m^2 \phi^2 - (1-\eta)\xi\kappa^2 \dot{\phi}^2 \right\}. \quad (2.19)$$

The expectation values of X^2 and χ^2 are expressed as

$$\langle X^2 \rangle = \frac{1}{2\pi^2} \int k^2 |X_k|^2 dk, \quad \langle \chi^2 \rangle = \frac{1}{2\pi^2} \int k^2 |\chi_k|^2 dk. \quad (2.20)$$

Introducing the function $Y_k = a^{3/2} X_k$, instead of X_k , we find

$$\ddot{Y}_k + \omega_k^2 Y_k = 0, \quad (2.21)$$

where

$$\omega_k^2 = \frac{k^2}{a^2} + G(\langle \chi^2 \rangle) - \frac{3}{4} \left(\frac{2\ddot{a}}{a} + \frac{\dot{a}^2}{a^2} \right), \quad (2.22)$$

which is a time dependent frequency of Y_k .

At the first stage of preheating when χ -particles are produced by quantum fluctuation, we find the occupation number in Y_k -state by the Bogoliubov transformation as

$$n_k = \frac{\omega_k}{2} \left(|Y_k|^2 + \frac{|\dot{Y}_k|^2}{\omega_k^2} \right) - \frac{1}{2}. \quad (2.23)$$

However, after many χ -particles are created and each mode is amplified, the χ_k field could be regarded as the classical field in a good approximation [13,14]. We may not have to use Eq. (2.23) at the classical stage. Khlebnikov and Tkachev developed the semiclassical description of fluctuation produced by the inflaton decay [12]. In fact, they studied the inflaton decay by the classical equation of motion and performed a fully nonlinear calculation. To give the initial conditions, we follow their approach, i.e. the initial distribution for Y_k is described as

$$P[Y_k; t = 0] = \sqrt{\frac{2\omega_k(0)}{\pi}} \exp[-2\omega_k(0)|Y_k|^2], \quad (2.24)$$

and \dot{Y}_k is correlated to Y_k as

$$\dot{Y}_k = -i\omega_k(0)Y_k. \quad (2.25)$$

We investigate the $\langle \chi^2 \rangle$ evolution with those initial conditions as the semiclassical problem.

From Eq. (2.19), we easily find that properties of the preheating in the non-minimal coupling theory are quite different from ordinary g -resonance. First, $\xi\kappa^2 m^2 \phi^2$ term and $\xi\kappa^2 \dot{\phi}^2$ term cause the resonance as well as interaction term $g^2 \phi^2$ with inflaton field. These different types of resonant terms either strengthen or weaken the resonance each other, depending on the coupling constants. Secondly, as the χ -particles are produced significantly, the suppression effect by the second term in Eq. (2.19) becomes crucial. This means that in case of non-minimal coupling, we have to consider not only ordinary back reaction effects to the inflaton field and metric but also the suppression effect by this term. In what follows, we will investigate these issues in detail.

III. THE RESONANCE BY POSITIVE COUPLING ξ

In this section, we investigate $g = 0$, $\xi > 0$ case. First, however, we briefly review the ordinary g -resonance, i.e., the case with $g \neq 0$, $\xi = 0$ for comparison [5,8]. In this and next two sections, we mainly study the massless χ field. For the massive case, we will give some discussion in the end of each section.

If the back reaction of the χ field to the inflaton field and metric are neglected, the inflaton field oscillates almost coherently with damping factor $3H$ and is approximately described as

$$\phi = \Phi(t) \sin mt. \quad (3.1)$$

The amplitude $\Phi(t)$ decreases with time as

$$\Phi(t) = \frac{M_{\text{PL}}}{\sqrt{3\pi mt}}. \quad (3.2)$$

Then the time-dependent frequency of the each component Y_k becomes

$$\omega_k^2 = \frac{k^2}{a^2} + g^2 \phi^2 = \frac{k^2}{a^2} + g^2 \Phi^2 \sin^2 mt. \quad (3.3)$$

We can reduce Eq. (2.21) to the well known Mathieu equation

$$\frac{d^2 Y_k}{dz^2} + [A_k - 2q \cos 2z] Y_k = 0, \quad (3.4)$$

where $z = mt$ and

$$A_k = 2q + \frac{\bar{k}^2}{a^2}, \quad (3.5)$$

$$q = \frac{g^2 \Phi^2}{4m^2}. \quad (3.6)$$

\bar{k} is normalized by m as $\bar{k} = k/m$. Stability or instability with Eq. (3.4) depends on the variables of A_k and q , which is shown by a stability-instability chart (see Fig. 1) [28]. In the unstable region (the lined region in Fig. 1), Y_k grows exponentially as $Y_k \propto \exp(\mu_k z)$ with the Floquet index μ_k and particles with momentum k are produced. For small q , the width of the instability band is small and few k -modes grow by this resonance. This is called the narrow resonance. On the other hand, for the large q , the resonance can occur for a broad range of the momentum k -space. Since the growth rate μ of the χ -particle becomes larger as the increase of the variable q , this resonance gives more efficient particle production than narrow one. This is called the broad resonance. Note that initial amplitude Φ of

the inflaton field and coupling constant g play important roles to decide whether resonance is narrow or broad. In the g -resonance case, the allowed region on the Mathieu chart is determined by the Eq (3.5) as

$$A_k \geq 2q. \quad (3.7)$$

Hence the broadest resonance is given by the limit line $A_k = 2q$.

When q is sufficiently large initially, the resonance of each mode occurs *stochastically* [5,8]. In this case, the frequency ω_k decreases by cosmic expansion and ω_k dramatically changes within each oscillation of the inflaton field, so the phases of χ field at successive moment of $\phi = 0$ are not correlated each other. At the first stage of the resonance, the fields cross large number of instability bands. The periods when they are in the instability band are so short that the resonance can not occur efficiently compared with that in the Minkowski spacetime. However, nevertheless, the number of χ -particles can still grow exponentially. As q becomes smaller, the universe expansion slows down, and the fields stay in each resonance band for a longer time. When q drops down to about 1, the first instability band

$$1 - q - \frac{1}{8}q^2 \leq A_k \leq 1 + q - \frac{1}{8}q^2, \quad (3.8)$$

becomes important. When the variables decrease below the lower boundary of Eq. (3.8) by the expansion of the Universe, the resonance terminates. We have to note here that there is another mechanism which terminates the resonance. When the initial value of q is large ($g \gtrsim 3.0 \times 10^{-4}$), χ -particles are produced efficiently and the back reaction onto the inflaton field cannot be ignored. This makes the oscillation of the inflaton field incoherent and finally stops the resonance. That is called the back reaction effect of the χ field.

Now we turn to the case of $g = 0, \xi > 0$. In this case the resonance occurs by the coupling between the χ field and the spacetime curvature R [23]. The $G(\langle\chi^2\rangle)$ term defined by Eq. (2.19) becomes

$$G(\langle\chi^2\rangle) = \frac{1}{(1-\eta)[1-(1-6\xi)\eta]} \left[2\xi\kappa^2 m^2 \phi^2 - (1-3\eta)\xi\kappa^2 \dot{\phi}^2 \right] + \frac{\eta}{1-\eta} \frac{4+(1-6\xi)(1-5\eta)}{1-(1-6\xi)\eta} \left\{ 2\xi\kappa^2 m^2 \phi^2 - (1-\eta)\xi\kappa^2 \dot{\phi}^2 \right\}. \quad (3.9)$$

We easily find that if η increases up to the order of unity, $G(\langle\chi^2\rangle)$ diverges and the frequency of (2.22) increases to infinity. The resonance seems to continue effectively at the final stage of preheating. However, this is not the case. Our numerical calculation shows that the resonance terminates when η is much smaller than unity in any cases. With the condition of $\eta \ll 1$, $G(\langle\chi^2\rangle)$ is rewritten as

$$G(\langle\chi^2\rangle) \approx \frac{\xi\kappa^2 m^2}{(1+6\xi\eta)^2} \left(2\phi^2 - \frac{\dot{\phi}^2}{m^2} \right). \quad (3.10)$$

Note that there exists the suppression factor $(1 + 6\xi\eta)^{-2}$, which makes the amplitude of the χ field small effectively. Even in the case of $\eta \ll 1$, we can expect that this suppression plays an important role when ξ takes large values. We will see later that this effect becomes significant in the case of $\xi \gtrsim 70$. When η is small compared with unity, the back reaction to the inflaton field and the metric is negligible and we find from Eq. (2.13) that the φ field oscillates almost coherently.

By using these relations, we can rewrite the equation of Y_k in the form of the Mathieu equation

$$\frac{d^2 Y_k}{dz^2} + [A_k - 2q \cos(2z - \alpha)] Y_k = 0, \quad (3.11)$$

where

$$A_k = \frac{\bar{k}^2}{a^2} + \frac{2p}{(1 + 6\xi\eta)^2}, \quad (3.12)$$

$$q = \frac{\sqrt{(2p)^2 + 2(\xi\kappa^2\Phi^2)^2}}{2(1 + 6\xi\eta)^2}, \quad (3.13)$$

$$p = \frac{\xi\kappa^2}{4} (\Phi^2 - \Phi'^2), \quad (3.14)$$

$$\alpha = \tan^{-1} \left(\frac{\xi\kappa^2\Phi\Phi'}{2p + \xi\kappa^2\Phi^2} \right). \quad (3.15)$$

A prime denotes a derivative with respect to z . Eq. (3.11) is not exactly the Mathieu equation, because it contains the time dependent phase term α . This term is due to the existence of $\dot{\phi}^2$ term in Eq. (3.10). If we define a new dimensionless time parameter $\bar{t} = mt/2\pi$, α is rewritten as

$$\alpha = \tan^{-1} \left(\frac{-4\pi\bar{t}}{12\pi^2\bar{t}^2 - 1} \right), \quad (3.16)$$

where we used the relation (3.2). Since \bar{t} represents the number of the oscillation of the inflaton field naively, α approaches zero rapidly within the first oscillation of the inflaton field. As a result, the time dependence of α does not affect the resonance process.

Although the equation of Y_k has the same form as the ordinary g -resonance except for the time-dependent phase α , properties of resonance are not the same. After the first oscillation of the inflaton field, setting an initial time as $\bar{t} = 1/4$ as Kofman et al. [8], we have the condition

$$\Phi \gg \frac{\dot{\Phi}}{m}. \quad (3.17)$$

Then the evolution of A_k and q is approximated as:

$$A_k \approx \frac{2}{3}q + \frac{\bar{k}^2}{a^2}, \quad (3.18)$$

$$q \approx \frac{3}{4(1+6\xi\eta)^2} \xi \kappa^2 \Phi^2 \approx \frac{1}{(1+6\xi\eta)^2} \frac{\xi}{2\pi^2 \bar{t}^2}. \quad (3.19)$$

The line described by Eq. (3.18) lies below the one which is obtained in the ordinary g -resonance. As is studied in [23], the Ricci scalar can be replaced with $\dot{\phi}^2$ term and non-minimal coupling provides another contribution. This is because the above relation (3.18) becomes different from the relation (3.5) of ordinary g -resonance. In fact, we can easily estimate that without $\dot{\phi}^2$ term, ξ must be larger than 10^4 for the effective resonance, because we have only the similar coupling term to the g -resonance in that case. Since the width of the instability bands are thick for large q (see Fig. 1), ξ -resonance gives broader resonance and we may expect the efficient χ -particle production. However, as is found from Eq. (3.19), there are two factors which decrease the variable q . One is the decrease of Φ by the expansion of the Universe and the other is the suppression effect caused by the factor $(1+6\xi\eta)^{-2}$, which appears only in the ξ -resonance. Which factor is more important depends on the parameter ξ and the efficiency of the resonance, i.e., η . When $\xi\eta \lesssim 0.1$, this suppression effect can be neglected. Note that the back reaction effect is negligible because η is always small in any parameter. Hence, it may be worth stressing that the ξ -resonance in the $g=0$ case will terminate only by passing through the resonance band, because the coherence of the inflaton is not broken.

By the final value of q ($=q_f$) when the resonance ends, we can estimate the time t_f when the resonance stops and the total amount of created χ -particles $\langle \bar{\chi}^2 \rangle_f \equiv \langle \chi^2 \rangle_f / m^2$. In the case of $q \gtrsim 1$, particle creation occurs when the frequency ω_k changes non-adiabatically, which condition is written as

$$\omega_k^2 < \frac{d\omega_k}{dt}. \quad (3.20)$$

Neglecting the $\dot{\Phi}$ in calculation in the $\xi \kappa^2 \dot{\phi}^2$ term in Eq. (3.10), ω_k^2 yields

$$\omega_k^2 \approx \frac{k^2}{a^2} + \frac{\xi \kappa^2 m^2}{(1+6\xi\eta)^2} (3\phi^2 - \Phi^2), \quad (3.21)$$

and then the non-adiabatic condition (3.20) becomes

$$\frac{k^2}{a^2} < \left[\frac{3\xi \kappa^2 m^2}{(1+6\xi\eta)^2} \phi \dot{\phi} - \frac{6\xi^2 \dot{\eta} \kappa^2 m^2}{(1+6\xi\eta)^3} (3\phi^2 - \Phi^2) \right]^{2/3} - \frac{\xi \kappa^2 m^2}{(1+6\xi\eta)^2} (3\phi^2 - \Phi^2). \quad (3.22)$$

Let us investigate the value of ϕ when the r.h.s. in Eq. (3.22) takes the maximum value. Non-adiabatic amplification occurs mostly when ϕ is passing through around the minimum of its potential ($|\phi| \ll M_{\text{PL}}$), so we can set $\dot{\phi} \approx m\dot{\Phi}$ in

Eq. (3.22). Moreover, $\dot{\eta}$ term is negligible compared with the former term, which is confirmed by numerical calculation.

Then, Eq. (3.22) can be approximately rewritten as

$$\frac{k^2}{a^2} < \left[\frac{3\xi\kappa^2 m^3}{(1+6\xi\eta)^2} \Phi\phi \right]^{2/3} - \frac{\xi\kappa^2 m^2}{(1+6\xi\eta)^2} (3\phi^2 - \Phi^2). \quad (3.23)$$

Differentiating the r.h.s. of Eq (3.23) with respect to ϕ , we find that it takes the maximal value at

$$\phi_{max} = \frac{1}{3^{3/4}} \sqrt{\frac{m\Phi}{C^{1/2}}} \approx \frac{1}{2} \sqrt{\frac{m\Phi}{C^{1/2}}}, \quad (3.24)$$

where $C \equiv 3\xi\kappa^2 m^2 / (1+6\xi\eta)^2$. Then the maximum value of momentum yields

$$\frac{\bar{k}_{max}^2}{a^2} = \frac{C\Phi^2}{3m^2} + \left(2^{4/3} - 1\right) \frac{\sqrt{C}\Phi}{4m}, \quad (3.25)$$

where $\bar{k}_{max}^2 \equiv k_{max}^2 / m^2$. As we have the relation $\sqrt{C}\Phi/m = 2\sqrt{q}$ by Eq. (3.19), the maximum momentum is rewritten in terms of q as

$$\frac{\bar{k}_{max}^2}{a^2} = \frac{4}{3}q - \left(2^{1/3} - \frac{1}{2}\right) \sqrt{q} \approx \frac{4}{3}q + \frac{3}{4}\sqrt{q}. \quad (3.26)$$

This equation gives the maximum momentum for the resonance. While the resonance terminates when the variables A_k and q pass the curve of

$$A_k \approx 1 - q - \frac{1}{8}q^2, \quad (3.27)$$

in the Mathieu chart [28]. Combining the relations (3.18), (3.26) and (3.27), we obtain the equation with respect to q_f as

$$q_f^2 + 24q_f + 6\sqrt{q_f} + 8 = 0, \quad (3.28)$$

resulting $q_f = 0.2165 \approx 1/5$. If we adopt the typical momentum k_* , which would be defined as

$$k_* = \frac{k_{max}}{\sqrt{2}}, \quad (3.29)$$

in stead of k_{max} , we find

$$3q_f^2 + 56q_f + 9\sqrt{q_f} + 24 = 0, \quad (3.30)$$

and $q_f = 0.3353 \approx 1/3$.

The analytic expression of Eq. (3.28) or (3.30) is only an approximation because the maximal momentum k_{max} will be changed when q drops down to $q \lesssim 1$. However, it gives good agreement with numerical calculation. First, we examine the evolution of $\langle \chi^2 \rangle$, comparing the results of numerical calculation with the analytical estimation. For $\xi \lesssim 10$, numerical calculation shows no effective production of $\langle \chi^2 \rangle$. This means that the initial value of q is so small and it decreases so fast because of the expansion of the Universe that the χ -field does not stay in the instability bands for enough time. For $10 \lesssim \xi \lesssim 70$, the resonance occurs because the period during which the χ field stays in the broad resonance band becomes longer. For example, in the case of $\xi = 50$, the value of $\langle \chi^2 \rangle$ first increases exponentially by the passage of time and reaches to its maximum value $\langle \bar{\chi}^2 \rangle_f = 3.090 \times 10^3$ at $\bar{t}_f = 2.85$ (Fig. 2(a)). Although $\langle \bar{\chi}^2 \rangle_f$ is not large enough for the efficient preheating, the parametric resonance evidently occurs. Since the maximal value of $\xi\eta$ is $\xi\eta_f \approx 1.9 \times 10^{-4}$, we can ignore the suppression factor $(1 + 6\xi\eta)^{-2}$ in Eq. (3.19). Hence the resonance is terminated by the expansion of the Universe. The final value of q obtained by the numerical calculation is $q_f \approx 0.312$, which is almost the same as the analytically estimated value with the typical momentum k_* . In the case that the suppression effect is neglected, we can estimate the time when the resonance ceases by

$$\bar{t}_f = \sqrt{\frac{\xi}{2\pi^2 q_f}} \approx \sqrt{\frac{3\xi}{2\pi^2}}. \quad (3.31)$$

For the case of $\xi = 50$, $\bar{t}_f = 2.76$, which is close to the numerical value $\bar{t}_f = 2.85$. After $\langle \bar{\chi}^2 \rangle$ reaches its maximum value, it decreases monotonically. This is the adiabatic damping due to the expansion of the Universe.

In order to see the ξ -dependence of the numbers of created particles, we depict $\langle \bar{\chi}^2 \rangle_f$ in terms of ξ in Fig. 3. It shows that although the created particle first increases as the coupling constant ξ gets large, it rather decreases beyond a critical value ξ_c , which can be understood as follows.

When ξ is less than about 100, $\langle \bar{\chi}^2 \rangle_f$ increases as the coupling constant ξ gets larger. This is just because the initial value of q is larger and then the resonance begins in the broader bands. For $70 \lesssim \xi \lesssim 200$, the suppression factor becomes important. The $\xi = 100$ case is shown in Fig. 2(b). At the first stage, $\langle \bar{\chi}^2 \rangle$ increases rapidly with the larger growth rate than the case with $\xi = 50$, but it reaches its maximal value $\langle \bar{\chi}^2 \rangle_f = 9.550 \times 10^5$ soon. Since $\xi\eta_f = 0.240$ at the maximum point, the suppression effect by $(1 + 6\xi\eta)^{-2}$ cannot be ignored. In Fig. 3, we find that $\langle \bar{\chi}^2 \rangle_f$ is almost flat around $\sim 10^6$ in the parameter range $\xi = 100 \sim 200$.

For $\xi \gtrsim 200$, the suppression effect by large ξ is more effective than increasing of $\langle \bar{\chi}^2 \rangle$. At the first stage of preheating, the growth rate of $\langle \bar{\chi}^2 \rangle$ becomes larger as the increase of ξ (Fig. 2(c)). However, the resonance soon

terminates with the smaller final value $\langle \bar{\chi}^2 \rangle_f$ than in the case of $\xi \approx 100$ by the suppression effect. For example, in the case with $\xi = 1000$, $\langle \bar{\chi}^2 \rangle_f = 8.318 \times 10^4$ and $\xi\eta_f = 2.090$ at $\bar{t}_f = 1.31$, which is much smaller than the amount in the case with $\xi = 100$. In fact, $\langle \bar{\chi}^2 \rangle_f$ decreases monotonically by the suppression effect beyond $\xi_c \sim 100$ -200 (Fig. 3). In the case of $\xi \gtrsim 200$, we can estimate the value of $\langle \bar{\chi}^2 \rangle_f$ as follows. Assuming that the mode with the typical momentum k_* is the leading mode of the growth of $\langle \bar{\chi}^2 \rangle$, we can rewrite Eq. (3.19) as

$$\langle \bar{\chi}^2 \rangle_f = \frac{(M_{\text{PL}}/m)^2}{48\pi\xi^2} \left(\sqrt{\frac{3\xi}{2\pi^2\bar{t}_f^2}} - 1 \right), \quad (3.32)$$

at the maximal point. In our numerical calculation, we find that \bar{t}_f is well approximated by the constant value 1.31 when ξ is greater than 500. Then, $\langle \bar{\chi}^2 \rangle_f$ decreases as

$$\langle \bar{\chi}^2 \rangle_f \propto \xi^{-3/2}, \quad (3.33)$$

which is confirmed by our numerical result given in Fig. 3 for $\xi \gtrsim 500$.

In Table I, we also show our numerical results and the estimated values (3.32) for the maximal value $\langle \bar{\chi}^2 \rangle_f$. The present analytical estimation gives a good approximation to the numerical results. A small difference between those may be due to the naive condition of Eq. (3.20). If we take into account all momenta larger than k_* , we will obtain the larger values of $\langle \bar{\chi}^2 \rangle_{\text{analytic}}$, which estimation gives closer value to the numerical one.

Finally, we should mention the effect of a mass of the χ -field. In general, the mass effect of the χ -field works as a suppression factor, because the relation between A_k and q in (3.12) is modified as

$$A_k = \frac{\bar{k}^2}{a^2} + \frac{2p}{(1 + 6\xi\eta)^2} + \frac{m_\chi^2}{m^2}. \quad (3.34)$$

However, since the resonance band is wider in ξ -resonance compared with g -resonance, the effective production of χ -particles is still expected even if the mass term is taken into account. In fact we have found that if the mass is order 10^{13} GeV (namely the same order of the inflaton mass), χ -particles are created as same as the massless case when ξ is about $100 \sim 200$. The example is given in Fig. 4. The final value of $\langle \bar{\chi}^2 \rangle$ in the case of $g = 0, \xi = 200, m_\chi = m$ is about 10^6 , which is almost the same of the massless case. However, for $\xi < 1000$, it is difficult to have a resonant production of χ -particles with the mass larger than $100m (\sim 10^{15} \text{ GeV})$, because the relation between A_k and q deviates from the resonance bands due to the mass term. When ξ is much larger than 1000, although it is not likely, we still expect production of massive χ -particle whose mass is of order 10^{15} GeV at the initial stage of preheating. However, as the production of χ -particle proceeds, $\xi\eta$ suppression becomes efficient for such a large value of ξ , resulting in a small

total amount of $\langle \bar{\chi}^2 \rangle$. Namely, massive χ -particle production is possible when ξ is sufficiently large, but the final amount of χ -particle gets small by the $\xi\eta$ suppression effect. Whether or not such a small amount of production can still provide us the baryonsynthesis is another problem, which we do not investigate here.

IV. THE RESONANCE BY NEGATIVE COUPLING ξ

Next, we investigate the case of $g = 0, \xi < 0$. Since η is small compared with unity as we will see later by numerical calculation, we can use the Mathieu equation (3.11) \sim (3.15) to analyze our numerical results in this case as well. Neglecting $\dot{\Phi}$ term, the relation between A_k and q is now

$$A_k \approx -\frac{2}{3}q + \frac{\bar{k}^2}{a^2}, \quad (4.1)$$

where

$$q \approx \frac{1}{(1 + 6\xi\eta)^2} \frac{|\xi|}{2\pi^2 t^2}. \quad (4.2)$$

Note that A_k can take a negative value because of the negative coupling ξ . This fact makes the properties of resonance quite different from the case of $\xi > 0$ as was pointed out in Ref. [23]. In the regions of $A_k < 0$, a new instability band (zeroth instability band) extends below some curve which is approximated by $A_k \approx -q^2/2$ when q is small (see Fig. 1). One of the important features is that this zeroth instability band reaches $A_k = 0$ in the limit of $q = 0$. Consider the modes with very small momentum k . The line of $A_k = -2q/3$ crosses to the curve $A_k \approx -q^2/2$ at $q \approx 1.4$. Hence, even if q evolves below unity by the expansion of the Universe, there remain some unstable modes in this instability band. Since the Floquet index μ_k of this instability band behaves as $\mu_k \sim \sqrt{q}$ when q is small, resonance continues to occur until q vanishes. Moreover, most of the $A_k < 0$ region is covered by either the zeroth or higher instability bands. Almost all modes contribute to the resonant process in almost all the time with high growth rate. Hence one can expect the very effective particle production.

We show numerical results for the evolution of $\langle \chi^2 \rangle$ in Fig. 5. For $\xi = -20$, q takes initially the value ~ 16 and modes are either in the first or in higher instability bands, depending on the momentum. However, after the first oscillation of the inflaton field, q decreases to ~ 1 and some modes enter into the zeroth instability band. $\langle \chi^2 \rangle$ increases exponentially mainly by those modes during the first several oscillations of the inflaton field. Thereafter the growth rate becomes small and $\langle \chi^2 \rangle$ approaches the constant value $\langle \bar{\chi}^2 \rangle_f = 4.1 \times 10^7$. At this stage, the production of χ -particle balances with the dilution by the Hubble expansion. For $\xi = -100$, $\langle \chi^2 \rangle$ increases more rapidly than the

case of $\xi = -20$ at the first stage and reaches to its maximum value $\langle \bar{\chi}^2 \rangle_f = 4.4 \times 10^6$ at $\bar{t} = 7.7$. The main growth of $\langle \chi^2 \rangle$ occurs until $\bar{t} = 2$, when q is of order 1. After $\bar{t} = 2$, the χ -field enters the zeroth instability band, and the increase of $\langle \chi^2 \rangle$ stops at $\bar{t} = 7.7$. After that, $\langle \chi^2 \rangle$ takes almost a constant value. This behavior is universal for the case with $\xi < 0$. To understand the present results more deeply, we shall estimate the value of $\langle \bar{\chi}^2 \rangle_f$.

From the relations (2.16) and (2.20), we can obtain the following relation:

$$\begin{aligned} \frac{d}{dt} \langle \chi^2 \rangle &= \sqrt{\frac{\langle \chi^2 \rangle}{\langle F^2 \rangle \langle X^2 \rangle}} \frac{1}{a^3} \left(\frac{d}{dt} \langle Y^2 \rangle - 3H \langle Y^2 \rangle \right), \\ &= \sqrt{\frac{\langle \chi^2 \rangle \langle X^2 \rangle}{\langle F^2 \rangle}} m (2\mu - 3\bar{H}), \end{aligned} \quad (4.3)$$

where we have used the expression $\langle Y^2 \rangle = a^3 \langle X^2 \rangle \sim e^{2\mu t}$ with μ being the Floquet index and $\bar{H} = H/m$. The growth of $\langle \chi^2 \rangle$ stops when the r.h.s. vanishes, i.e., when the dilution effect by expansion of the Universe surpasses the particle creation rate. Neglecting the back reaction effect on the metric, the evolution of the Hubble parameter is approximately written by

$$\bar{H} \approx \sqrt{\frac{4\pi}{3}} \frac{\Phi}{M_{\text{PL}}} \approx \frac{1}{3\pi\bar{t}}. \quad (4.4)$$

While, the relation between μ and A in the zeroth instability band can be written by [28]

$$\mu \approx \left[-A + \frac{(A-1)q^2}{2(A-1)^2 - q^2} \right]^{1/2}. \quad (4.5)$$

Considering the modes which are close to the line of $A = -2q/3$, the Floquet index μ is given as

$$\mu \approx \sqrt{\frac{2q}{3}} \approx \frac{1}{1+6\xi\eta} \sqrt{\frac{|\xi|}{3}} \frac{1}{\pi\bar{t}}. \quad (4.6)$$

Until $\langle \chi^2 \rangle$ reaches to its maximum value, μ decreases faster than $1/\bar{t}$ by the existence of the suppression factor $1/(1+6\xi\eta)$. Because of this behavior, the Hubble expansion, which decreases as $\sim 1/\bar{t}$, will catch up with the inflaton decay, and then the preheating is terminated. Namely, the main factor which stops the growth of $\langle \chi^2 \rangle$ is the production of $\langle \chi^2 \rangle$ itself. Substituting Eqs. (4.4), (4.6) to Eq. (4.3), the growth rate of $\langle \chi^2 \rangle$ is approximately given as

$$\frac{d}{dt} \langle \chi^2 \rangle \approx \sqrt{\frac{\langle \chi^2 \rangle \langle X^2 \rangle}{\langle F^2 \rangle}} \frac{m}{\pi\bar{t}} \left[\frac{1}{1+6\xi\eta} \sqrt{\frac{4|\xi|}{3}} - 1 \right]. \quad (4.7)$$

When the term in the square bracket vanishes, the growth of $\langle \chi^2 \rangle$ ceases. By this condition we find the final value of $\langle \chi^2 \rangle$ as

$$\langle \bar{\chi}^2 \rangle_f = \frac{(M_{\text{PL}}/m)^2}{48\pi\xi^2} \left[\sqrt{\frac{4|\xi|}{3}} - 1 \right]. \quad (4.8)$$

Note that the final value of $\langle \chi^2 \rangle$ depends on only ξ , but not on \bar{t}_f . Once $\langle \chi^2 \rangle$ reaches to its maximum, μ and H both decreases as $1/\bar{t}$. Note that in the case of $g = 0, \xi > 0$, the dependence of μ is $\mu \sim q \sim 1/\bar{t}^2$ when q is close to zero and that $\langle \chi^2 \rangle$ does not approach to constant value but adiabatically decreases by the Hubble expansion.

From Eq. (4.7), we find that the resonance does not occur in the case of $0 < |\xi| < 0.75$, and this is confirmed by numerical calculation. In this parameter range, the growth rate μ is small as compared with the Hubble expansion rate. By Eq. (4.8), we guess that $\langle \bar{\chi}^2 \rangle_f$ may take the maximal value at $\xi \approx -1.33$. However, this is not the case actually. In $-3 \lesssim \xi \lesssim -1$ case, since the creation rate of χ -particle is small, it takes much time to complete the χ -particle production. As time passes, a contribution of produced χ -particles to the Hubble expansion rate becomes comparable to that of the inflaton field, and the estimation (4.8) can not be applied. The growth of $\langle \bar{\chi}^2 \rangle$ stops before $\xi\eta$ suppression effect in Eq. (4.7) becomes significant. Hence for $-3 \lesssim \xi \lesssim -1$, although the χ -particle production is possible, the final abundance of χ -particle is not so large. For example, in $\xi = -2$ case, the numerical value of the final abundance is $\langle \bar{\chi}^2 \rangle_f = 3.2 \times 10^3$, which is much smaller than the estimated value $\langle \bar{\chi}^2 \rangle_f = 1.0 \times 10^9$ by Eq. (4.8). On the other hand, for $\xi \lesssim -3$, $\xi\eta$ suppression effect plays a crucial role to terminate the increase of $\langle \bar{\chi}^2 \rangle$. Numerically, $\langle \bar{\chi}^2 \rangle_f$ takes maximal value $\langle \bar{\chi}^2 \rangle_{max} \sim 3.2 \times 10^8$ at $\bar{t}_f \sim 3.3 \times 10^5$ when $\xi \sim -4$. In this case, although the growth rate is still small compared with other cases as $g > 0, \xi = 0$ and $g = 0, \xi > 0$, the final fluctuation is large. For $\xi \lesssim -4$, $\langle \bar{\chi}^2 \rangle$ continues to grow until χ -particles are significantly produced, and finally $\xi\eta$ suppression effect terminates the resonance. In these cases, the analytic estimation based on Eq. (4.8) can be applied. By Eq. (4.8), we expect that $\langle \bar{\chi}^2 \rangle_f$ decreases as the decrease of ξ ($\lesssim -4$). For example, numerical values of the final fluctuation are $\langle \bar{\chi}^2 \rangle_f = 1.122 \times 10^8$ for $\xi = -10$ and $\langle \bar{\chi}^2 \rangle_f = 4.130 \times 10^7$ for $\xi = -20$. In $\xi = -10$ case, \bar{t}_f is about $\bar{t}_f \sim 1.0 \times 10^3$ and the growth rate is $\mu \sim 0.001$. For $\xi = -20$, the growth rate increases up to $\mu \sim 0.1$, and the resonance ends at $\bar{t}_f = 28.28$. In the case of $|\xi| \gg 1$, the resonant time becomes very short by this suppression and the final value of $\langle \bar{\chi}^2 \rangle$ is reduced. Eq. (4.8) shows that $\langle \bar{\chi}^2 \rangle_f$ decreases as $|\xi|^{-3/2}$ for $|\xi| \gg 1$.

In TABLE II, we show the analytically estimated and numerical values of $\langle \bar{\chi}^2 \rangle_f$ for various cases. We find that the analytical estimation gives good agreement for $\xi \lesssim -4$. The small discrepancy comes from the fact that we mainly considered the modes close to $k = 0$, which gives the largest contribution in most of the stages. Also, since the actual Hubble parameter is larger than is estimated by Eq. (4.4), this decreases the estimated value of $\langle \bar{\chi}^2 \rangle_f$. Note that the final value of $\langle \bar{\chi}^2 \rangle_f = 3.162 \times 10^8$ at $\xi = -4$ is larger than the maximal value in the case of $g = 0, \xi > 0$ ($\langle \bar{\chi}^2 \rangle_{max} \sim 10^6$ at $\xi = 100 \sim 200$). Since the resonance bands of negative coupling are broader than those of positive coupling in

previous section, the more χ -particles are created and the final value of $\langle \bar{\chi}^2 \rangle$ becomes larger. However, when the value of $|\xi|$ becomes large, $\langle \bar{\chi}^2 \rangle_f$ decreases as $|\xi|^{-3/2}$, which is the same as positive coupling case. We conclude that the suppression effect controls the final value of $\langle \bar{\chi}^2 \rangle$ for large $|\xi|$ in ξ -resonance case.

When the mass of χ -field is taken into account, the resonance is suppressed as the case of $g = 0, \xi > 0$. However, since the resonance band is broader than those of $g = 0, \xi > 0$ case, we expect considerable production of χ -particles for $\xi < 0$. One important property in negative ξ case is that massive χ -particle is hard to be created once χ -field enters the zeroth instability band. This is because χ -field deviates from the zeroth instability region by the mass effect. Even in the case of $\xi = -20 \sim -30$ when massless χ -particles are effectively produced as $\langle \bar{\chi}^2 \rangle_f \gtrsim 5 \times 10^7$, massive χ -particle production is strongly suppressed because χ -field deviates from the zeroth instability band soon after the first oscillation of the inflaton field. For example, in the case of $g = 0, \xi = -30, m_\chi = m$, we find $\langle \bar{\chi}^2 \rangle_f \sim 10^3$, which is not an effective resonance. Rather, in the case of $g = 0, \xi = -100 \sim -200$, in spite of the $\xi\eta$ suppression effect, the produced χ -particles exceed more than $\langle \bar{\chi}^2 \rangle_f = 10^6$ for $m_\chi = m$ (Fig. 6). However, if $m_\chi \gtrsim 10m$, it becomes difficult to produce more than $\langle \bar{\chi}^2 \rangle_f \sim 10^6$ even for $\xi = -100 \sim -200$. We show in Fig. 7 the final abundance of χ -particle as a function of m_χ for $\xi = -1000$ case. In this case, we find that χ -particle whose mass is more than $m_\chi \sim 100m$ can not be created. In order to produce the GUT scale particles ($m_\chi \sim 10^3 m \sim 10^{16}$ GeV), the value of A_k is more than $A_k = 10^6$ since $m_\chi^2/m^2 \sim 10^6$ in Eq. (3.34). This means that the resonance does not happen at all from the very beginning unless $\xi \lesssim -10^6$ [Note $q \approx |\xi|$ initially]. Moreover, when $|\xi|$ is extremely large such as $\xi \sim -10^6$, χ -particle with the mass of order 10^{16} GeV can be created initially, but the final amount will be largely reduced by the $\xi\eta$ suppression effect. As is the same with $g = 0, \xi > 0$ case, whether or not such a small amount of production can provide us the baryonsynthesis is another problem. We then conclude that for massive case, effective χ -particle production is expected when the χ field does not deviate from instability bands initially and $\xi\eta$ suppression effect is not too strong.

V. THE COMBINED RESONANCE

In previous two sections, we have shown that the non-minimal coupling will give rise to the parametric resonance depending on the value of coupling constant ξ . Here we shall investigate a combination of g -resonance and ξ -resonance (the combined resonance). When $g \neq 0$, $g^2 \langle \chi^2 \rangle$ term in the equation for the inflaton field (2.13) becomes important at the final stage of the evolution and changes the effective mass of the inflaton field. By this back reaction effect,

the production of χ -particles is suppressed. Similarly, produced χ -particles will affect the metric by the coupling between the χ and inflaton fields. However, first, in order to examine the naive structure of the present system, we shall rewrite the equation for the χ field under the condition of $g^2\langle\chi^2\rangle \ll m^2$ and $\eta \ll 1$. With Eqs. (3.1) and (3.2), the equation for the χ field is reduced to the form of Mathieu equation (3.11) with (3.12), (3.15), and q and p being defined as

$$q = \frac{\sqrt{(2p)^2 + (g^2\Phi^2/m^2 + 2\xi\kappa^2\Phi^2)\xi\kappa^2\Phi^2}}{2(1 + 6\xi\eta)^2}, \quad (5.1)$$

$$p = \frac{1}{4} \left(\frac{g^2\Phi^2}{m^2} + \xi\kappa^2\Phi^2 - \xi\kappa^2\Phi'^2 \right). \quad (5.2)$$

With the condition (3.17), A_k and q are rewritten as

$$A_k \approx \frac{\bar{k}^2}{a^2} + 2q \frac{g^2\Phi^2/m^2 + \xi\kappa^2\Phi^2}{|g^2\Phi^2/m^2 + 3\xi\kappa^2\Phi^2|} \approx \frac{\bar{k}^2}{a^2} + 2q \frac{g^2 + 8\pi\xi(m/M_{\text{PL}})^2}{|g^2 + 24\pi\xi(m/M_{\text{PL}})^2|}, \quad (5.3)$$

$$q \approx \frac{1}{4(1 + 6\xi\eta)^2} \left| \frac{g^2\Phi^2}{m^2} + 3\xi\kappa^2\Phi^2 \right| \approx \frac{(M_{\text{PL}}/m)^2}{48\pi^3(1 + 6\xi\eta)^2 t^2} \left| g^2 + 24\pi\xi \left(\frac{m}{M_{\text{PL}}} \right)^2 \right|. \quad (5.4)$$

On the Mathieu chart, there are two quantities which determine the efficiency of the resonance. One is the initial value q_i . This determines the Floquet index, i.e., the growth rate of the χ -particle. It becomes large as g and ξ get large as seen from Eq. (5.4). In general, if we can neglect the back reaction effect, we expect more efficient resonance for large q_i . Another quantity is the gradient of the line on which the variables A_k and q trace during evolution of the system. It determines how many modes contribute to resonance. In the present case, the gradient is given by the ratio of ξ to g^2 . In the minimal coupling case, $\xi = 0$, so the typical line is $A_k = 2q$. In the non-minimal case, however, there are several types of lines which show different behaviors. Then we shall first classify the Mathieu chart into several regions by changing ξ/g^2 from ∞ to $-\infty$ (see Fig. 8). When $\xi/g^2 = \infty$, the resonance is the similar to the positive ξ -resonance discussed in Sec. III. When $0 < \xi/g^2 < \infty$, the resonance occurs below the $A_k = 2q$ line. We call the resonance in this parameter region “new-broad resonance”. When $\xi = 0$, resonance occurs only by g -coupling: $A_k = 2q + \bar{k}^2/a^2$ and the ordinary g -resonance is recovered. If ξ becomes negative, A_k and q enter the region of $A_k > 2q$, and we call the resonance in this parameter region “ordinary-broad resonance”. When $\xi/g^2 = -(M_{\text{PL}}/m)^2/24\pi$, q vanishes and no resonance occurs. As ξ/g^2 decreases further, the gradient gets smaller and the resonance becomes broader again. When $\xi/g^2 = -(M_{\text{PL}}/m)^2/16\pi$, the typical line is $A_k = 2q$, which is same as the ordinary g -resonance in spite of the existence of ξ -coupling. The parameter range $-(M_{\text{PL}}/m)^2/12\pi < \xi/g^2 < -(M_{\text{PL}}/m)^2/16\pi$, corresponds to the region between $A_k = 2q$ and $A_k = 2q/3$, and the system enters the new-broad resonance region again. As ξ/g^2 gets

smaller further, A_k and q enter the region of $A_k < 2q/3$. We call the resonance in this region “wide resonance”. When $\xi/g^2 < -(M_{\text{PL}}/m)^2/8\pi$, the gradient becomes negative. $\xi/g^2 = -\infty$ corresponds to the negative ξ -resonance discussed in the previous section. In what follows, we will examine each cases one by one in detail paying attention to which parameter range in ξ -coupling assists the g -resonance.

Before proceeding the individual investigation, we shall give some criteria for the back reaction effect on the inflaton field and for the suppression effect by $\xi\eta$ term.

1. For the back reaction effect on the inflaton field, we shall adopt the criterion

$$g^2 \langle \bar{\chi}^2 \rangle \lesssim 0.1. \quad (5.5)$$

If the $\langle \bar{\chi}^2 \rangle$ exceeds this criterion, the back reaction becomes important. In the case of $g \neq 0, \xi = 0$, our numerical analysis shows that this criterion corresponds to the condition of $g \lesssim 3 \times 10^{-4}$.

2. For the $\xi\eta$ suppression effect, we adopt the criterion

$$\xi\eta \lesssim 0.1. \quad (5.6)$$

We will see that those effects are crucial for the effective χ -particle creation at the final stage of preheating.

A. $\xi > 0$ (new-broad resonance)

This case corresponds the parameter range,

$$\frac{2}{3}q + \frac{\bar{k}^2}{a^2} < A_k < 2q + \frac{\bar{k}^2}{a^2}, \quad (5.7)$$

on the Mathieu chart (Fig. 8(a)) and the resonance band is broad compared with usual g -resonance case. We shall discuss the following three cases separately.

1. $g \ll 3 \times 10^{-4}$ case

In the case of $\xi = 0$, i.e. the ordinary g -resonance, the width of the instability bands are small when $g \ll 3 \times 10^{-4}$. The χ -particles are actually created only in the first instability band, and the resonance occurs in the narrow band from the beginning. As a result, χ -particle is not produced efficiently. By taking ξ -coupling into account, however, the resonance is assisted since initial value of q becomes larger and the resonance band becomes broader as seen from

Eqs. (5.3) and (5.4). In order to obtain $\langle \bar{\chi}^2 \rangle_f \sim 10^6$, we need the coupling constant $\xi = 100 \sim 200$. Because the resonance occurs mainly by ξ -coupling, the properties of resonance is almost the same as $g = 0, \xi > 0$ case. For fixed value ξ , we find that g makes the resonance band narrower and the resonance less effective, although it makes the initial value of q larger. In fact, the numerical calculation shows that $\langle \bar{\chi}^2 \rangle_f$ with g is smaller than that without g and its growth rate of $\langle \bar{\chi}^2 \rangle$ is also smaller. In this sense, g -coupling weakens the ξ -resonance. In this parameter region, the back reaction effect on the inflaton mass is negligible and the suppression by $\xi\eta$ term terminates the χ -particle production.

2. $g \sim 3 \times 10^{-4}$ case

In this case, we find from Fig. 9 that the resonance is divided into two stages as in the ordinary g -resonance, namely first broad resonance regime and following narrow resonance regime. We put the suffix “ b ” to the variables just after the broad resonance regime as \bar{t}_b and q_b . Although the resonance starts from the broad resonance region even in the $\xi = 0$ case, the resonance band becomes broader by adding the ξ -coupling. Furthermore, the initial value of q becomes large as seen in Eq. (5.4). Since more modes contribute to the resonance, both the growth rate of $\langle \bar{\chi}^2 \rangle$ and the value of $\langle \bar{\chi}^2 \rangle_b$ get larger (see Fig. 9 and Table III). This means that the ξ -coupling supports the g -resonance well in the broad resonance regime. After the resonance enters the narrow resonance regime ($\bar{t} \approx 8$), the growth rate hardly depends on ξ . At the final stage, however, we cannot neglect the suppression effect by the $\xi\eta$ term. As ξ becomes large, the variables A_k and q cross the lower boundary of the first instability band at an earlier time and the final value of $\langle \bar{\chi}^2 \rangle_f$ is suppressed a little compared with that in the ordinary g -resonance. In this case, the back reaction effect is marginally less important.

3. $g > 3 \times 10^{-4}$ case

In this parameter region, the back reaction to the inflaton field should be taken into consideration. In the case of $\xi = 0$, χ -particles are produced quite effectively in the broad resonance regimes and $\langle \bar{\chi}^2 \rangle_f$ takes maximal value $\langle \bar{\chi}^2 \rangle_{max} \approx 5.0 \times 10^7$ for $g \approx 1 \times 10^{-3}$, in which case the initial value of q ($q_i \approx 1.075 \times 10^4$) is large enough as estimated by Eq. (5.4). As g increases, the back reaction term $g^2 \langle \bar{\chi}^2 \rangle$ gives significant effect even small value of $\langle \bar{\chi}^2 \rangle$ and $\langle \bar{\chi}^2 \rangle_f$ rather decreases. Even if we take ξ -coupling into account, it does not change the growth rate at the first stage of the resonance very much when g is large (see Fig. 10). For example, in the case of $g = 1.0 \times 10^3$ and

$\xi = 100$, the initial value estimated by Eq. (5.4) is $q_i \approx 1.083 \times 10^4$. This is almost same as the case of $\xi = 0$. Furthermore, the relation between A_k and q is $A_k \approx 1.99q + \bar{k}^2/a^2$, which shows also the same broadness. Hence the initial stage of the resonance is governed by the g -coupling. In order to find the effect of the ξ -coupling, we may set ξ very large ($\xi \gtrsim 10^4$ for $g = 1 \times 10^{-3}$). Such a large ξ coupling, however, causes extremely strong suppression and we do not expect the efficient resonance. In the final stage, either the suppression effect by $\xi\eta$ or the back reaction effect terminates the resonance depending on the coupling constants g and ξ . Generally speaking, when ξ takes a large value, the suppression factor becomes important before the created χ -particles cause the significant back reaction. By two criteria (5.5) and (5.6), we can estimate a rough dependence. Once the created particles exceed one of the criteria first, the resonance will terminate. Since the r.h.s. of these criteria are the same, comparing the l.h.s. terms, two effects become equivalent when

$$g^2 = 8\pi \left(\frac{m}{M_{\text{PL}}} \right)^2 \xi^2. \quad (5.8)$$

Hence, if $g^2 > 8\pi(m/M_{\text{PL}})^2\xi^2$, the back reaction terminates the resonance. Otherwise, the resonance is terminated by the suppression effect. This estimation has been confirmed by the numerical calculations. As a result, it is difficult to create χ -particles more than $\langle \bar{\chi}^2 \rangle_f \sim 5.0 \times 10^7$ even if ξ -coupling is taken into account.

B. $-(M_{\text{PL}}/m)^2/16\pi < \xi/g^2 < 0$ (ordinary-broad resonance)

As we can see by Eq. (5.3), both terms of g and ξ suppress the instability in this case. The gradient of the q - A_k line becomes steep, and this parameter range corresponds to the region between the line of $A_k = 2q + \bar{k}^2/a^2$ and A_k axis in the Mathieu chart. This means that the resonance occurs in narrower bands than that in the case of $\xi = 0$. In particular, for $\xi/g^2 = -(M_{\text{PL}}/m)^2/24\pi$, the variable q vanishes. Since the width of any instability bands vanishes for $A_k > 0$, the resonance does not occur at all although both g -coupling and ξ -coupling exist. As for the initial value of q , both terms of g and ξ suppress it as seen from Eq. (5.4). As a result ξ -coupling always suppresses g -resonance in any parameter range. This effect is remarkable when q is small. However, for large g , ξ terms is negligible because both the gradient of the q - A_k line and q_i depend on square of g while they depend linearly on ξ . Hence the properties of the resonance are almost the same as those in ordinary g -resonance if $g > 3.0 \times 10^{-4}$ and $0 < |\xi| < 100$.

C. $-(M_{\text{PL}}/m)^2/12\pi < \xi/g^2 < -(M_{\text{PL}}/m)^2/16\pi$ (new-broad resonance)

This parameter range corresponds to the regions between $A_k = 2q + \bar{k}^2/a^2$ and $A_k = 2q/3 + \bar{k}^2/a^2$ on the Mathieu chart (Fig. 8(b)). The resonance gives the same broadness as the case discussed in the subsection A. However, there is a different point in an efficiency of the resonance. In the present case, q evolves in the range of

$$\frac{1}{(1 + 6\xi\eta)^2} \frac{|\xi|}{6\pi^2 \bar{t}^2} < q < \frac{1}{(1 + 6\xi\eta)^2} \frac{|\xi|}{4\pi^2 \bar{t}^2}. \quad (5.9)$$

Comparing this with the Eq. (3.19) in the case of $g = 0, \xi > 0$, q in Eq. (5.9) is smaller than that in the case of $g = 0$ by factor 2-3 for the fixed value of $|\xi|$. Remembering that for $g = 0, \xi > 0$ the value of ξ must be $\xi \gtrsim 100$ to achieve $\langle \bar{\chi}^2 \rangle_f \sim 10^6$, we can estimate that $|\xi|$ is needed at least $|\xi| \gtrsim 200$ for the efficient resonance in the case of $\xi/g^2 \approx -(M_{\text{PL}}/m)^2/12\pi$. This means that the parameters which cause the effective resonance are a little more restrictive than the ξ -resonance discussed in Sec. III. In the case of $\xi/g^2 \approx -(M_{\text{PL}}/m)^2/16\pi$, q evolves on the line $A_k \approx 2q + \bar{k}^2/a^2$ and the broadness of the resonance bands is similar to the ordinary g -resonance. For this reason, we need the value of $|\xi|$ that is more than 10000 for the effective resonance, but such a large $|\xi|$ causes the strong $\xi\eta$ suppression and the final value of $\langle \chi^2 \rangle$ is reduced. We show the numerical results on the $A_k = 2q/3$ line in Table IV, have confirmed the above analysis. If $|\xi|$ is less than 100, the resonance hardly occurs. For example, when $\xi = -100$ and $g = 6.140 \times 10^{-5}$, the final value of $\langle \bar{\chi}^2 \rangle$ is $\langle \bar{\chi}^2 \rangle_f = 5.0 \times 10$. On the other hand, in the case of $\xi = -200$ and $g = 7.089 \times 10^{-5}$, the final value is $\langle \bar{\chi}^2 \rangle_f = 1.0 \times 10^5$. g -resonance is in fact assisted by ξ -coupling in this case. However, it is difficult to produce the χ -particles more than $\langle \bar{\chi}^2 \rangle_f \sim 10^6$ in this parameter range.

D. $-\infty < \xi/g^2 < -(M_{\text{PL}}/m)^2/12\pi$ (wide resonance)

This parameter range corresponds to the regions between $A_k = 2q/3 + \bar{k}^2/a^2$ and $A_k = -2q/3 + \bar{k}^2/a^2$ (Fig. 8(b)). Since the contribution from the negative ξ -coupling surpasses the g -coupling, the resonance band becomes quite broad as ξ/g^2 decreases. For $-(M_{\text{PL}}/m)^2/8\pi < \xi/g^2 < -(M_{\text{PL}}/m)^2/12\pi$, the gradient of the q - A_k line is positive and the resonance terminates when the variables q and A_k cross the lower boundary of the first instability band as the former cases. After the resonance terminates, $\langle \bar{\chi}^2 \rangle$ decreases gradually by the adiabatic expansion. We show the result of the numerical calculations in the $\xi/g^2 = -(M_{\text{PL}}/m)^2/8\pi$ case, which correspond to $A_k = 0$, in Table V. In the case of $|\xi| \lesssim 50$, resonance does not occur because the initial value of q is too small. However as $|\xi|$ becomes large, $\langle \bar{\chi}^2 \rangle_f$

increases and for $\xi = -200$ and $g = 7.089 \times 10^{-5}$, $\langle \bar{\chi}^2 \rangle_f = 1.0 \times 10^6$. From these results we can conclude that resonance is more effective than the previous case.

When $\xi/g^2 \lesssim -(M_{\text{PL}}/m)^2/8\pi$, the q - A_k line passes through the zeroth instability band near its boundary. Since the Floquet index is small there, it takes long time to reach the final value of $\langle \bar{\chi}^2 \rangle$ even for the large $|\xi|$. $\langle \bar{\chi}^2 \rangle_f$ is determined by the balance between the creation rate of the χ -particle and the expansion rate of the Universe (Eq. (4.8)). As ξ/g^2 approaches to $-\infty$, the properties of the resonance are almost the same as the case of $g = 0, \xi < 0$, and then ξ -coupling assists g -resonance. Since the existence of g -coupling makes the growth rate small for fixed value of ξ , resonance is most efficient in the case of $g = 0$.

E. summary

We shall summarize the properties of the resonance and the suppression effect. On the ξ - g diagram (Fig. 11), we show which suppression factor is significant in various coupling regimes. We can easily find that the back reaction effect is dominant in the case of $g \gtrsim 3 \times 10^{-4}$ and $g \gtrsim 5 \times 10^{-6}|\xi|$ (the lined region in Fig. 11). However, in the case of $g \lesssim 3 \times 10^{-4}$ and $|\xi| \gg 1$, the $\xi\eta$ suppression effect becomes more important. In fact, $\xi\eta$ suppression appears either for $\xi \gtrsim 100$ or $\xi/g^2 \lesssim -0.1(M_{\text{PL}}/m)^2$ (the shaded region in Fig. 11). In the parameter range like $-(M_{\text{PL}}/m)^2/12\pi < \xi/g^2 < -(M_{\text{PL}}/m)^2/16\pi$ (new-broad resonance with $\xi < 0$ case), however, although $|\xi|$ is of order 100, the effective χ -particle production will not be expected. In the region where the back reaction or suppression effect becomes significant, we may expect a large amount of particle production, although it will be reduced for extremely large $|\xi|$.

In Fig. 12, we show $\langle \bar{\chi}^2 \rangle_f$ in terms of ξ and g in 3-dimensional plane. From this figure, we find three plateaus; one corresponds to the back reaction region with large g , and the other two correspond to $\xi\eta$ suppression regions shown in Fig. 11. $\langle \bar{\chi}^2 \rangle_f$ takes maximal value of $\langle \bar{\chi}^2 \rangle_{max} \approx 3.2 \times 10^8$ at $g \lesssim 1 \times 10^{-5}, \xi \approx -4$. In other regions, we find that the numerical result agrees well with our analysis.

In this section, we have studied the combined resonance of g and ξ . For $g \gtrsim 3 \times 10^{-4}$, when the back reaction effect is important, the final values of $\langle \bar{\chi}^2 \rangle$ does not become larger than those of g -resonance significantly even if ξ -coupling is taken into account. This is due to both of the $\xi\eta$ suppression and the back reaction. In the case that $|\xi|$ is large as $|\xi| \gtrsim 100$, the $\xi\eta$ suppression effect becomes more important than the back reaction. For $g \lesssim 3 \times 10^{-4}$, g -resonance is sometimes assisted by ξ -coupling. For example, for $100 \lesssim \xi \lesssim 200$ and $-\infty < \xi/g^2 < -(M_{\text{PL}}/m)^2/16\pi$,

ξ -coupling assists g -resonance. In particular, for $g \lesssim 1 \times 10^{-5}$, the resonance structure is almost the same as the case of $g = 0, \xi \neq 0$, which means that it is essentially the ξ -resonance.

VI. CONCLUSIONS AND DISCUSSIONS

In this paper we have examined the properties of resonance with non-minimally coupled scalar field χ in preheating phase. We have found that effective resonance is possible only by a non-minimal coupling $\xi R\chi^2$ in a certain range of parameter ξ . In the case of $g = 0, \xi > 0$, the relation of A_k and q in the Mathieu chart is $A_k = 2q/3 + \bar{k}^2/a^2$ and the resonance band becomes broader in comparison with g -resonance ($A_k = 2q + \bar{k}^2/a^2$). This is due to the existence of $\xi\kappa^2\dot{\phi}^2$ term and the structure of resonance is different from that of g -resonance. Without $\xi\kappa^2\dot{\phi}^2$ term, ξ must be larger than 10^4 for the effective resonance. However, as we have shown here, the effective resonance is possible for $\xi \sim O(100)$. For example in the case of $g = 0, \xi = 100$, we find $\sqrt{\langle\chi^2\rangle_f} \approx 10^{16}$ GeV, which is comparable to the case of $g \approx 3 \times 10^{-4}, \xi = 0$. The unique feature of ξ -resonance is the existence of $\xi\eta$ suppression effect. As ξ increases up to about 100, $\langle\chi^2\rangle_f$ also increases because χ -field stays in the broad resonance bands longer. However, when ξ exceeds about 100, $\xi\eta$ suppression effect by the production of χ -particles is significant and $\langle\chi^2\rangle_f$ does not increase for the case of $\xi \gtrsim 100$. Rather, beyond $\xi \sim 200$, $\langle\chi^2\rangle_f$ decreases by $\xi\eta$ suppression effect as $\langle\chi^2\rangle_f \propto \xi^{-3/2}$. In the case of $g = 0, \xi > 0$, we find that the maximal value of $\langle\chi^2\rangle_f$ is $\sqrt{\langle\chi^2\rangle_{max}} \approx 10^{16}$ GeV at $\xi = 100 \sim 200$.

As for the case of $g = 0, \xi < 0$, the relation between A_k and q becomes $A_k = -2q/3 + \bar{k}^2/a^2$ and the resonance band is further broader than the case of $g = 0, \xi > 0$. The important difference from other cases is that A_k - q curve will pass through the zeroth instability band below the curve of $A_k = -q^2/2$. As a result, even if q decreases under unity by expansion of the Universe, the modes close to $k = 0$ always stay in the resonance band. In this case, we find the termination in the growth of $\langle\chi^2\rangle$ at which the growing rate μ of $\langle Y^2 \rangle$ balances the expansion rate of the Universe. In $-1 \lesssim \xi \lesssim 0$ case, the increase of $\langle\chi^2\rangle$ is not expected because the Hubble expansion rate surpasses the growing rate. In $-3 \lesssim \xi \lesssim -1$ case, although $\langle\chi^2\rangle$ increases as the passage of time, it takes much time to reach its maximum because μ is very small and resonance terminates before $\xi\eta$ suppression effect becomes significant. For $\xi \lesssim -3$, $\langle\chi^2\rangle_f$ takes rather large values and $\langle\chi^2\rangle_f$ takes maximal value $\sqrt{\langle\chi^2\rangle_{max}} \sim 2 \times 10^{17}$ GeV when $\xi \approx -4$. As ξ decreases from $\xi \lesssim -4$, although the growth rate μ increases, the final fluctuation of χ -particle decreases. This is because $\xi\eta$ suppression effect due to χ -particle production plays a crucial role to terminate the resonance. As a result, $\langle\chi^2\rangle_f$ decreases as $|\xi|^{-3/2}$ for $|\xi| \gg 1$. We should also note that the value of $\sqrt{\langle\chi^2\rangle_{max}}$ in the case of $g = 0, \xi < 0$ is

greater than that in the case of $g = 0, \xi > 0$. This is because the resonance bands for $\xi < 0$ are broader than those for $\xi > 0$.

We have also studied the combined resonance of interactions $g^2\phi^2\chi^2$ and $\xi R\chi^2$. The structure of resonance is quite different depending on two parameters of g and ξ . What we had been interested in is whether ξ -coupling assists g -resonance in any cases. However, we find that this is not the case. For $g \gtrsim 3 \times 10^{-4}$, and back reaction effect on the inflaton field and metric is important, g -resonance is not assisted by ξ -coupling because of $\xi\eta$ suppression effect as well as back reaction effect at the final stage of preheating. In the parameter range where χ -particles are significantly produced only by g -resonance, the maximal value of $\langle\chi^2\rangle_f$ does not increase even if we include the ξ -coupling. On the other hand, in the case of $g \lesssim 3 \times 10^{-4}$, ξ -coupling may assist g -resonance in the parameter ranges of $100 \lesssim \xi \lesssim 200$ and $-\infty < \xi/g^2 < -(M_{\text{PL}}/m)^2/16\pi$. In particular, for $g \lesssim 1 \times 10^{-5}$, the structure of resonance is almost the same as the case with $g = 0, \xi \neq 0$, and it is essentially the ξ -resonance. We find that the maximal value of $\sqrt{\langle\chi^2\rangle_f}$ is about 2×10^{17} GeV for $g \lesssim 1 \times 10^{-5}, \xi \approx -4$, which is larger than the minimally coupled case with $g \approx 1 \times 10^{-3}$.

There are several things we did not investigate in this paper. One of them is the rescattering effect. As χ -particles are produced significantly, the fluctuations of the inflaton field are also generated and would affect the production of χ -particles. Although it is expected that the structure of resonance does not change so much at the first stage of preheating, the rescattering effect will modify the final production of χ -particles because it becomes important at the final stage of preheating when χ -particles are significantly produced. As ϕ -particles are created, spatially inhomogeneity of the ϕ -field would prevent from the resonant production of χ -particles, resulting $\eta = \xi\kappa^2\langle\chi^2\rangle$ to be reduced. Then we may find either insufficient production of χ -particles or the same amount of χ -particles with a delay of time to reach the limiting value due to the $\xi\eta$ suppression. As for ϕ -particle creation through the present coupling, we did not investigate details at present. For complete study of preheating, however, we should consider the growth of ϕ -particles due to rescattering effect quantitatively beyond mean field approximation.

We did not consider the case when the coupling g^2 between ϕ and χ is negative, although it was pointed out in [29] that the production of χ -particles increases significantly compared with the positive coupling case. This is similar to the geometric reheating with negative ξ in the sense that A_k can take a negative value in the Mathieu chart. It may be interesting to study the combined resonance of negative g^2 and ξ .

In this paper, we have also not studied the metric perturbation in preheating phase. However, several authors pointed out that metric perturbation is influenced by the parametric resonance [30–33]. It was recognized the Bardeen

parameter is well conserved quantity in reheating phase except the short period when $\dot{\phi}$ is close to zero [30,33]. On the other hand, Bassett et al. [32] recently found that the rapid growth of metric perturbation by negative coupling instability is expected and this stimulates the growth of scalar field. It is worth investigating whether the growth of metric perturbation enhances the fluctuation of χ field non-minimally coupled to spacetime curvature R with $\xi < 0$.

We have studied a parametric resonance by ξ -coupling ($\xi R\chi^2$) as well as g -interaction ($g^2\phi^2\chi^2$). Although we expect that any scalar field will couple to spacetime curvature R through quantum effects, the value of ξ considered here may be too large. However, in other theories of gravity such as the Brans-Dicke theory [34], the induced gravity [35], and the higher-curvature theories [36], we may have different types of coupling to the spacetime curvature, which might give a natural mechanism for an effective resonance. These issues are under investigation.

ACKNOWLEDGEMENTS

We would like to thank Jun-ichirou Koga and Hiroki Yajima for useful discussions. T. T. is thankful for financial support from the JSPS. This work was supported partially by a Grant-in-Aid for Scientific Research Fund of the Ministry of Education, Science and Culture (No. 09410217 and Specially Promoted Research No. 08102010), by a JSPS Grant-in-Aid (No. 094162), and by the Waseda University Grant for Special Research Projects.

-
- [1] E. W. Kolb and M. S. Turner, *The Early Universe* (Addison-Wesley, Redwood City, California, 1990); A. D. Linde, *Particle Physics and Inflationary Cosmology* (Harwood, Chur, Switzerland, 1990).
- [2] A. D. Dolgov and A. D. Linde, Phys. Lett. **116B**, 329 (1982).
- [3] L. F. Abbott, E. Fahri, and M. Wise, Phys. Lett. **117B**, 29 (1982).
- [4] J. Traschen and R. H. Brandenberger, Phys. Rev. D **42**, 2491 (1990); Y. Shatanov, J. Traschen, and R. H. Brandenberger, Phys. Rev. D **51**, 5438 (1995).
- [5] L. Kofman, A. Linde, and A. A. Starobinsky, Phys. Rev. Lett. **73**, 3195 (1994).
- [6] D. Boyanovsky, H. J. de Vega, R. Holman, D. S. Lee, and A. Singh, Phys. Rev. D **51**, 4419 (1995); D. Boyanovsky, M. D'Attanasio, H. J. de Vega, R. Holman, D. S. Lee, and A. Singh, Phys. Rev. D **52**, 6805 (1995); D. Boyanovsky, H. J. de Vega, R. Holman, D. S. Lee, and A. Singh, J. F. J. Salgado, Phys. Rev. D **54**, 7570 (1996).
- [7] M. Yoshimura, Prog. Theor. Phys. **94**, 873 (1995); H. Fijisaki, K. Kumekawa, M. Yamaguchi, and M. Yoshimura, Phys. Rev. D **53**, 6805 (1996); H. Fijisaki, K. Kumekawa, M. Yamaguchi, and M. Yoshimura, Phys. Rev. D **54**, 2494 (1996).
- [8] L. Kofman, A. Linde, and A. A. Starobinsky, Phys. Rev. D **73**, 3258 (1997).
- [9] P. B. Green, L. Kofman, A. Linde, and A. A. Starobinsky, Phys. Rev. D **56**, 6175 (1997).
- [10] D. I. Kaiser, Phys. Rev. D **53**, 1776 (1995); D. I. Kaiser, Phys. Rev. D **56**, 706 (1997).
- [11] D. T. Son, Phys. Rev. D **54**, 3745 (1996).
- [12] S. Khlebnikov and I. I. Tkachev, Phys. Rev. Lett. **77**, 219 (1996).
- [13] S. Khlebnikov and I. I. Tkachev, Phys. Lett. **B390**, 80 (1997); S. Khlebnikov and I. I. Tkachev, Phys. Rev. Lett. **79**, 1607 (1997); S. Khlebnikov and I. I. Tkachev, Phys. Rev. D **56**, 653 (1997).
- [14] T. Prokopec and T. G. Roos, Phys. Rev. D **55**, 3768 (1997).
- [15] L. Kofman, A. Linde, and A. A. Starobinsky, Phys. Rev. Lett. **76**, 1011 (1996); I. I. Tkachev, Phys. Lett. **B376**, 35 (1996); S. Kasuya and M. Kawasaki, Phys. Rev. D **56**, 7597 (1997); S. Khlebnikov, L. Kofman, A. Linde, and I. I. Tkachev, Phys. Rev. Lett. **81**, 2012 (1998).
- [16] E. W. Kolb, A. D. Linde, and A. Riotto, Phys. Rev. Lett. **77**, 3716 (1996).
- [17] I. Affleck and M. Dine, Nucl. Phys. **B249**, 361 (1985).
- [18] R. D. Jordan, Phys. Rev. D **33**, 444 (1986).
- [19] E. Calzetta and B. L. Hu, Phys. Rev. D **35**, 495 (1987); E. Calzetta and B. L. Hu, Phys. Rev. D **37**, 2878 (1988).
- [20] J. Baacke, K. Heitmann, C. Pätzold, Phys. Rev. D **55**, 2320 (1997); J. Baacke, K. Heitmann, C. Pätzold, Phys. Rev. D **56**, 6556 (1997).
- [21] J. Schwinger, J. Math. Phys. **2**, 407 (1961); P. M. Bakshi and K. T. Mahanthappa, J. Math. Phys. **4**, 1 (1963); L. V. Keldysh, Sov. Phys. JETP **20**, 1018 (1965).
- [22] D. Boyanovsky, D. Cormier, H. J. de Vega, R. Holman, A. Singh, and M. Srednicki, Phys. Rev. D **56**, 1939 (1997); D. Boyanovsky, R. Holman, S. Prem Kumar, Phys. Rev. D **56**, 1958 (1997).
- [23] B. A. Bassett and S. Liberati, Phys. Rev. D **58** 021302 (1998).
- [24] In the self-coupling model such as $\lambda\phi^4$ interaction, a non-minimal coupling may not play any important role [10].
- [25] Wai-Mo Suen and Clifford M. Will, Phys. Lett. **B205**, 447 (1988).
- [26] T. Futamase and K. Maeda, Phys. Rev. D **39**, 399 (1989).
See also G. Magnano, M. Ferraris and M. Francaviglia, Gen. Rel. Grav. **19**, 465 (1987); M. Ferraris, M. Francaviglia and G. Magnano, Class. Quantum Grav. **7**, 261 (1990); A. Jakubiec and J. Kijowski, Phys. Rev. D **37**, 1406 (1988); K. Maeda, Phys. Rev. D **39**, 3159 (1989).
- [27] In the original frame (2.1), writing down the basic equations and adopting the mean field approximation, we find its gravity part as $(1 - \xi\kappa^2\langle\chi^2\rangle)G_{\mu\nu} = \dots$. To write down this basic equation in Einstein frame, we have to adopt the conformal factor $\Omega^2 = 1 - \eta$. Although the basic equations in the original frame with the mean field approximation can be obtained in above lines, those are very complicated. Instead, we start with the basic equations in the Einstein frame with the same conformal factor $\Omega^2 = 1 - \eta$. Although both basic equations are not exactly the same because of how to treat derivative terms of the mean field approximation of the χ field, these terms are not so important in our analysis. Then we expect that our results may still be reliable. In order to perform exact analysis, we have to solve the basic equations in the original frame by using lattice simulation.
- [28] N. W. Mac Lachlan, *Theory and Applications of Mathieu Functions* (Dover, New York, 1961).
- [29] P. B. Green, T. Prokopec, and T. G. Roos, Phys. Rev. D **58**, 6484 (1997).
- [30] H. Kodama and T. Hamazaki, Prog. Theor. Phys. **96**, 949 (1996); T. Hamazaki and H. Kodama, Prog. Theor. Phys. **96**, 1123 (1996).
- [31] Y. Nambu and A. Taruya, Prog. Theor. Phys. **97**, 83 (1997).
- [32] B. A. Bassett, D. I. Kaiser, and R. Maartens, hep-ph/9808404.
- [33] F. Finelli and R. Brandenberger, hep-ph/9809490.

- [34] C. Brans and R. H. Dicke, *Phys. Rev.* **124**, 925 (1961); D. La and P. J. Steinhardt, *Phys. Rev. Lett.* **62**, 376 (1989); A. Berkin, K. Maeda, J. Yokoyama, *Phys. Rev. Lett.* **65**, 141 (1990); J. D. Barrow and K. Maeda, *Nucl. Phys.* **B341**, 294 (1990); A. Berkin and K. Maeda, *Phys. Rev. D* **44**, 1691 (1991); A. D. Linde, *Phys. Lett.* **B238**, 160 (1990); A. D. Linde, *Phys. Rev. D* **49**, 748 (1994); J. Garcia-Bellido, A. D. Linde, and D. A. Linde, *Phys. Rev. D* **50**, 730 (1994).
- [35] A. Zee, *Phys. Rev. Lett.* **42**, 417 (1979); S. L. Adler, *Phys. Lett.* **95B**, 241 (1980); S. L. Adler, *Rev. Mod. Phys.* **54**, 729 (1982); F. S. Accetta, D. J. Zoller, and M. S. Turner, *Phys. Rev. D* **31**, 3046 (1985); J. L. Cervantes-Cota and H. Dehnen, *Nucl. Phys.* **B442**, 391 (1995); J. L. Cervantes-Cota and H. Dehnen, *Phys. Rev. D* **51**, 395 (1995).
- [36] K. S. Stelle, *Phys. Rev. D* **16**, 953 (1977); N. H. Barth and S. M. Christensen, *Phys. Rev. D* **28**, 1876 (1983); A. A. Starobinsky, *Phys. Lett.* **91B**, 99 (1980); A. A. Starobinsky, *Sov. Astron. Lett.* **10**, 135 (1984); K. Maeda, J. A. Stein-Schabes, and T. Futamase, *Phys. Rev. D* **39**, 2848 (1989); A. R. Liddle and D. H. Lyth, *Phys. Rep.* **231**, 1 (1993).

TABLE I. The final values $\langle \bar{\chi}^2 \rangle_f$ obtained by the analytical estimation and by the numerical calculation in the case of $g = 0, \xi > 0$. The analytical estimation gives a good approximation to the numerical results. $\langle \bar{\chi}^2 \rangle_{numerical}$ takes the maximal value at $\xi \sim 100$. We also show the time \bar{t}_f when the resonance ceases and $\xi\eta$ which indicates a suppression effect. For large ξ , the suppression effect ($q \sim (1 + 6\xi\eta)^{-2}$) becomes crucial.

ξ	\bar{t}_f	$\langle \bar{\chi}^2 \rangle_{analytic}$	$\langle \bar{\chi}^2 \rangle_{numerical}$	$\xi\eta_{numerical}$
20	1.85	—	8.610	8.7×10^{-8}
50	2.85	—	3.090×10^3	1.9×10^{-4}
70	2.85	—	3.750×10^5	4.6×10^{-2}
100	2.40	4.138×10^5	9.550×10^5	2.4×10^{-1}
500	1.31	1.513×10^5	2.109×10^5	1.3
1000	1.31	5.626×10^4	8.318×10^4	2.1
10000	1.31	1.922×10^3	2.630×10^3	6.6

TABLE II. The final value $\langle \bar{\chi}^2 \rangle_f$ obtained by the analytical estimation and by the numerical calculation in the case of $g = 0, \xi < 0$. For $|\xi| \geq 4$, both values show the same tendency that $\langle \bar{\chi}^2 \rangle_f$ gets large for decreasing $|\xi|$. However, for $|\xi| \leq 3$, the analytic estimation by Eq. (4.8) can not be applied (see text for the detail). $\langle \bar{\chi}^2 \rangle_{numerical}$ takes the maximal value at $\xi \approx -4$.

ξ	\bar{t}_f	$\langle \bar{\chi}^2 \rangle_{analytic}$	$\langle \bar{\chi}^2 \rangle_{numerical}$	$ \xi \eta_{numerical}$
-2	7.5×10^5	1.049×10^9	3.184×10^3	3.2×10^{-7}
-4	3.3×10^5	5.425×10^8	3.162×10^8	1.3×10^{-1}
-10	1.0×10^3	1.758×10^8	1.122×10^8	2.8×10^{-1}
-20	28.28	6.903×10^7	4.130×10^7	4.2×10^{-1}
-50	15.26	1.896×10^7	1.099×10^7	6.9×10^{-1}
-100	7.66	6.994×10^6	4.355×10^6	1.1
-1000	4.61	2.355×10^5	1.606×10^5	4.0
-10000	4.18	7.591×10^3	5.069×10^3	12.7

TABLE III. The numerical result for the broad resonance in the $g = 3 \times 10^{-4}$ case. \bar{t}_b and $\langle \bar{\chi}^2 \rangle_b$ are the values when the broad resonance regime ends. $\langle \bar{\chi}^2 \rangle_b$ gets larger for large ξ because the resonance band becomes very broad. However, $\langle \bar{\chi}^2 \rangle_f$ turns out to be smaller for large ξ because of the suppression effect, although it does not depend on ξ so much.

ξ	\bar{t}_b	$\langle \bar{\chi}^2 \rangle_b$	\bar{t}_f	$\langle \bar{\chi}^2 \rangle_f$
-20	6.26	3.019	14.36	2.951×10^5
0	6.26	5.495	14.36	7.244×10^5
50	6.26	3.162×10	12.85	6.309×10^5
100	6.26	2.344×10^2	11.88	4.570×10^5

TABLE IV. The numerical result for the new-broad resonance on the $A_k = 2q/3$ line on the Mathieu chart. g does not take large value for this parameter range of ξ . The effective resonance is expected only for $|\xi| > 200$.

ξ	g	$\langle \bar{\chi}^2 \rangle_f$
-20	2.745×10^{-5}	—
-50	4.341×10^{-5}	—
-70	5.137×10^{-5}	—
-100	6.140×10^{-5}	5.012×10
-200	7.089×10^{-5}	1.013×10^5

TABLE V. The numerical result for the wide resonance on the $A_k = 0$ line on the Mathieu chart. The resonance occurs mainly by the ξ -coupling. The effective resonance is expected only for $|\xi| > 100$.

ξ	g	$\langle \bar{\chi}^2 \rangle_f$
-20	2.241×10^{-5}	—
-50	3.545×10^{-5}	3.981
-70	4.194×10^{-5}	1.016×10^4
-100	5.013×10^{-5}	3.206×10^5
-200	7.089×10^{-5}	1.047×10^6

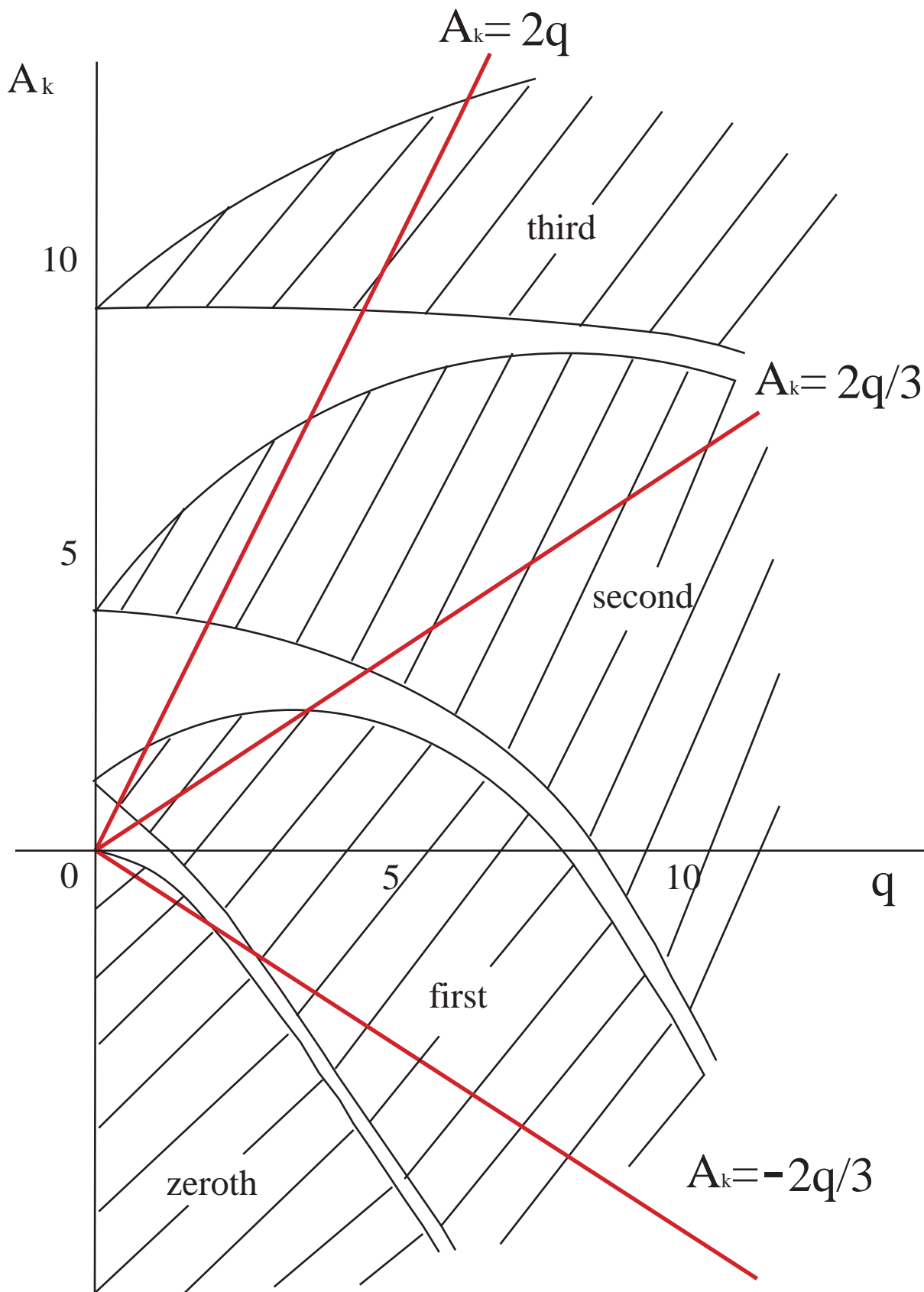
Figure Captions

- FIG. 1: The schematic diagram of the Mathieu chart and the typical paths for three types of resonance. The lined regions denote the instability bands (zeroth, first, second, \dots). The line of $A_k = 2q$ is the typical line of the ordinary g -resonance, while the lines of $A_k = 2q/3$ and $A_k = -2q/3$ show the lowest limits of the resonances by positive and negative ξ -couplings, respectively. We find that the width of the instability bands becomes wider for large q . The Floquet index in the lower instability band gets larger for fixed q .
- FIG. 2: The evolution of $\langle \bar{\chi}^2 \rangle$ as a function of \bar{t} in the case of $g = 0, \xi > 0$ ((a) $\xi = 50$, (b) $\xi = 100$ and (c) $\xi = 1000$). We find that the parametric resonance occurs by the positive ξ -coupling. $\langle \bar{\chi}^2 \rangle$ increases exponentially and reaches to its final value $\langle \bar{\chi}^2 \rangle_f$. After then, it decreases by the adiabatic expansion. $\langle \bar{\chi}^2 \rangle_f$ takes the maximal value for $\xi \sim 100$. For larger ξ ($\xi \gtrsim 100$), although the growth rate becomes large, the final value $\langle \bar{\chi}^2 \rangle_f$ is suppressed by the $\xi\eta$ term.
- FIG. 3: The final value of $\langle \bar{\chi}^2 \rangle$ as a function of ξ in the case of $g = 0, \xi > 0$. For $0 \lesssim \xi \lesssim 100$, $\langle \bar{\chi}^2 \rangle_f$ increases as ξ increases because the initial value of q gets large. For $100 \lesssim \xi \lesssim 200$, $\langle \bar{\chi}^2 \rangle_f$ takes its maximal value ($\sim 10^6$), and for $\xi \gtrsim 200$, $\langle \bar{\chi}^2 \rangle_f$ decreases by the suppression factor as $\sim \xi^{-3/2}$.
- FIG. 4: The evolution of $\langle \bar{\chi}^2 \rangle$ as a function of \bar{t} in the case of $g = 0, \xi = 200, m_\chi = m$. The significant production of massive χ -particles of order $m \sim 10^{13}$ GeV is expected by the positive ξ -resonance.
- FIG. 5: The evolution of $\langle \bar{\chi}^2 \rangle$ as a function of \bar{t} in the case of $g = 0, \xi < 0$ ((a) $\xi = -20$, (b) $\xi = -50$ and (c) $\xi = -100$). $\langle \bar{\chi}^2 \rangle$ increases exponentially in the first stage by the parametric resonance and reaches to its final value $\langle \bar{\chi}^2 \rangle_f$. After then, it approaches constant value because the creation rate of χ -particle and the expansion rate of the Universe balance.
- FIG. 6: The evolution of $\langle \bar{\chi}^2 \rangle$ as a function of \bar{t} in the case of $g = 0, \xi = -200, m_\chi = m$. The final value of $\langle \bar{\chi}^2 \rangle_f \approx 10^{6.5}$ is larger than the case of $g = 0, \xi = 200, m_\chi = m$.
- FIG. 7: The final value of $\langle \bar{\chi}^2 \rangle$ as a function of $\bar{m}_\chi = m_\chi/m$ in the case of $\xi = -1000$. $\langle \bar{\chi}^2 \rangle_f$ decreases as \bar{m}_χ increases, and parametric resonance can not be expected for $\bar{m}_\chi \gtrsim 100$ (namely, for $m_\chi \gtrsim 10^{15}$ GeV).
- FIG. 8: The relation between A_k and q in the case of the combined resonance of g and ξ . (a) As ξ/g^2 decreases from ∞ to $-(M_{\text{PL}}/m)^2/24\pi$, the relation changes from $A_k = 2q/3 + \bar{k}^2/a^2$ to $q = 0$ as the arrow in the figure. We call the resonance in each parameter region as follows. $0 < \xi/g^2 < \infty$: new-broad resonance, and $-(M_{\text{PL}}/m)^2/24\pi < \xi/g^2 < 0$: ordinary-broad resonance. (b) As ξ/g^2 decreases from $-(M_{\text{PL}}/m)^2/24\pi$ to $-\infty$, the relation changes from $q = 0$ to $A_k = -2/3q + \bar{k}^2/a^2$ as the arrow in the figure. We call the resonance in each parameter region as follows. $-(M_{\text{PL}}/m)^2/16\pi < \xi/g^2 < -(M_{\text{PL}}/m)^2/24\pi$: ordinary-broad resonance, $-(M_{\text{PL}}/m)^2/12\pi < \xi/g^2 < -(M_{\text{PL}}/m)^2/16\pi$: new-broad resonance, and $-\infty < \xi/g^2 < -(M_{\text{PL}}/m)^2/12\pi$: wide resonance.
- FIG. 9: The evolution of $\langle \bar{\chi}^2 \rangle$ as a function of \bar{t} in the case of $g = 3.0 \times 10^{-4}$ (a) $\xi = 0$, (b) $\xi = 50$ and (c) $\xi = 100$). We find that the resonance is divided into two stages; one of which is the first broad resonance stage and the other is the narrow one. The growth rate in the broad resonance stage becomes larger for larger ξ . However the final value $\langle \bar{\chi}^2 \rangle_f$ is suppressed by the $\xi\eta$ term.

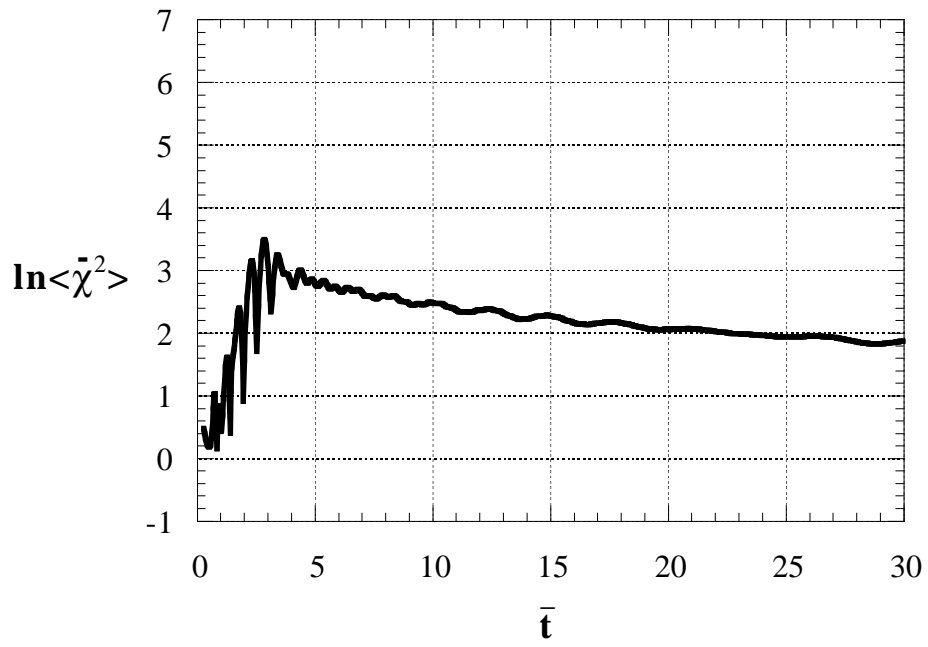
FIG. 10: The evolution of $\langle \bar{\chi}^2 \rangle$ as a function of \bar{t} in the case of $g = 1.0 \times 10^{-3}$ (a) $\xi = 0$, (b) $\xi = 50$ and (c) $\xi = 100$). The broad and narrow resonance stages are not distinguished. The growth rates are almost the same for each ξ , because the resonance occurs mainly by g -coupling. When $\langle \bar{\chi}^2 \rangle$ reaches its maximal value, the back reaction effect terminates the resonance.

FIG. 11: The structure of resonance, the back reaction and $\xi\eta$ suppression effects in terms of ξ and g . The regions [A], [B], [C], [D] denote new-broad resonance ($\xi > 0$), ordinary-broad resonance ($-(M_{\text{PL}}/m)^2/16\pi < \xi/g^2 < 0$), new-broad resonance ($-(M_{\text{PL}}/m)^2/12\pi < \xi/g^2 < -(M_{\text{PL}}/m)^2/16\pi$), wide resonance ($-\infty < \xi/g^2 < -(M_{\text{PL}}/m)^2/12\pi$) respectively. With this diagram, we easily understand the resonance structure. The lined regions ($g \gtrsim 3 \times 10^{-4}$ and $g \gtrsim 5 \times 10^{-6}|\xi|$) denote those where the back reaction effect is significant. The shaded regions ($g \lesssim 3 \times 10^{-4}$ and either $\xi \gtrsim 100$ or $\xi/g^2 \lesssim -0.1(M_{\text{PL}}/m)^2$) denote those where $\xi\eta$ suppression effect becomes important.

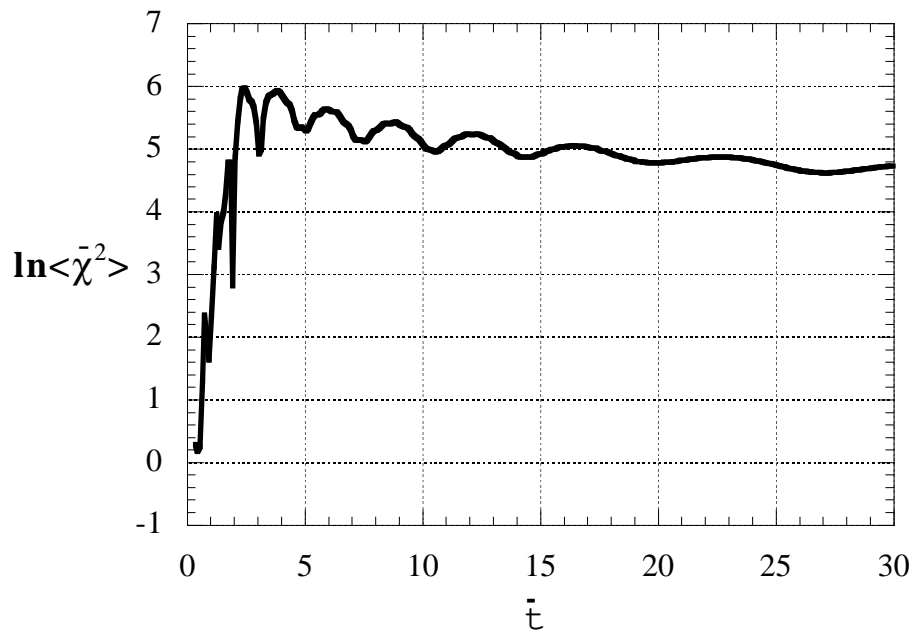
FIG. 12: $\langle \bar{\chi}^2 \rangle_f$ in terms of ξ and g . We find three plateaus, one of which $\langle \bar{\chi}^2 \rangle_f$ takes maximal value $\langle \bar{\chi}^2 \rangle_{max} \approx 3.2 \times 10^8$ for $g \lesssim 1 \times 10^{-5}, \xi \approx -4$.



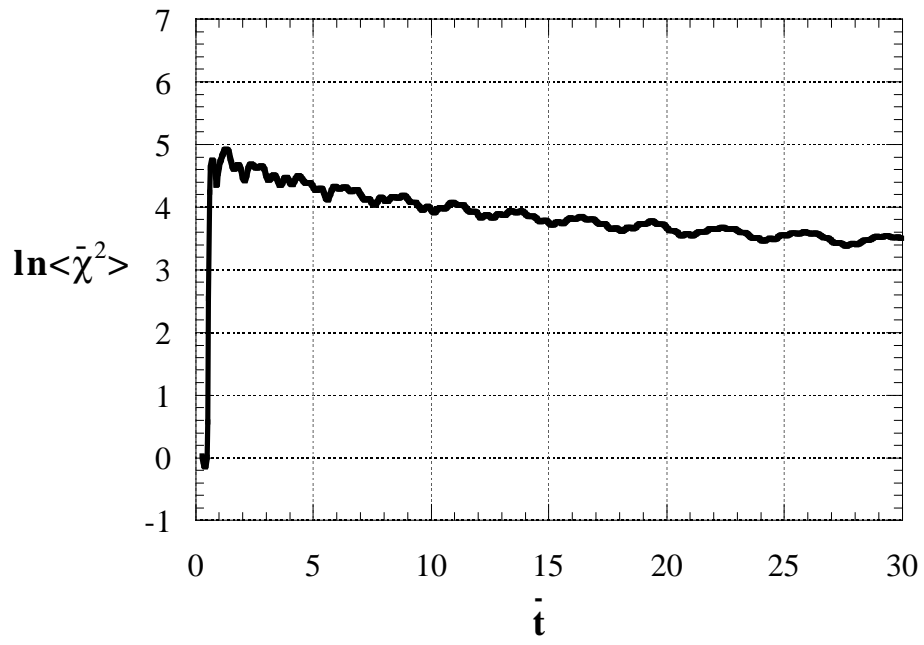
$g=0, \xi=50$



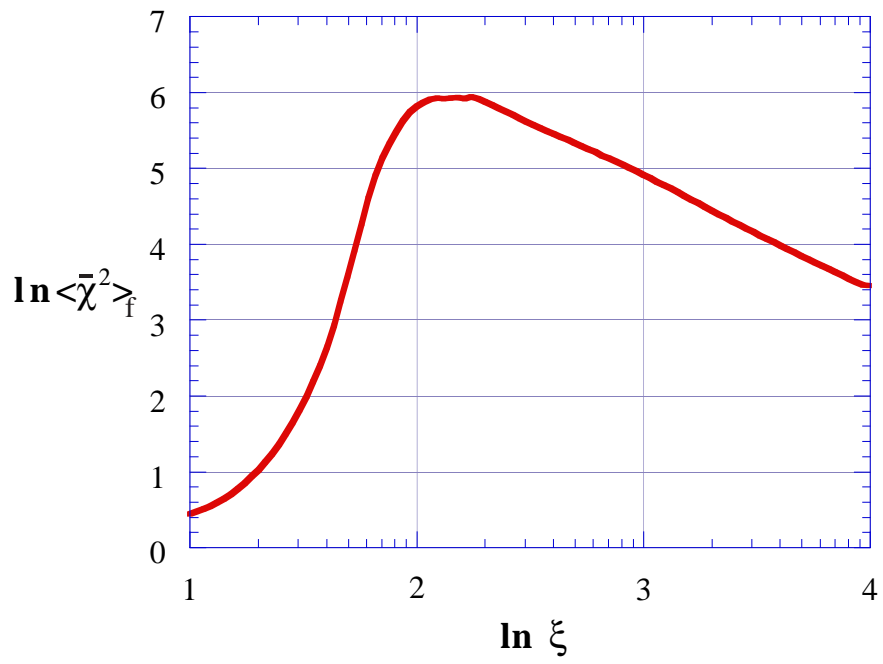
$g=0, \xi=100$



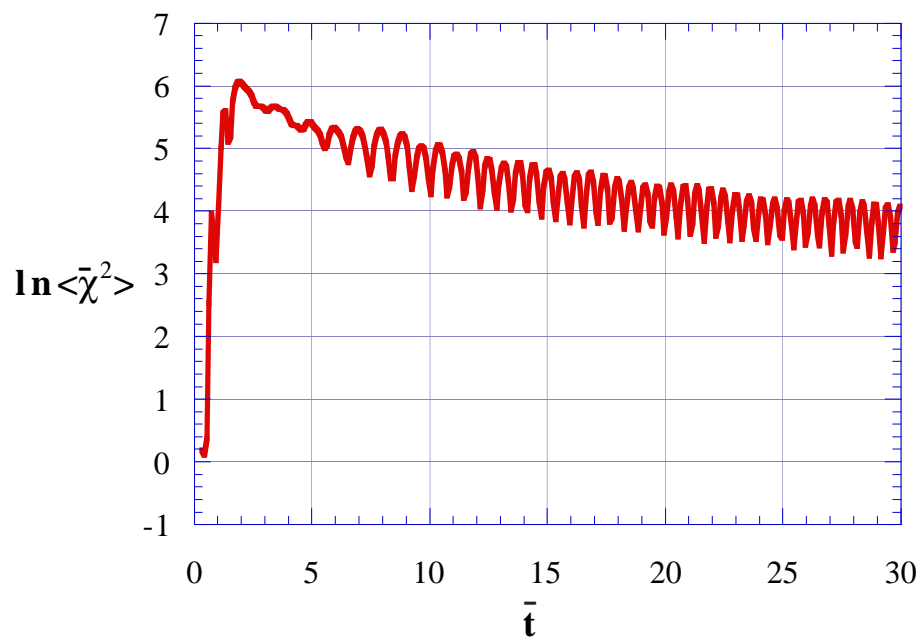
$g=0, \xi=1000$



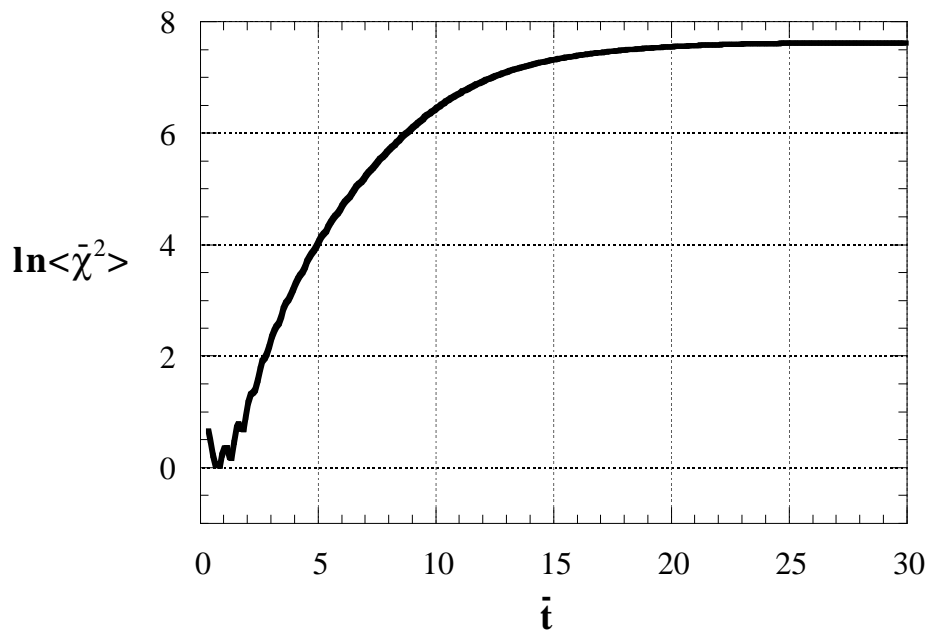
$\xi - \langle \chi^2 \rangle_f$ relation



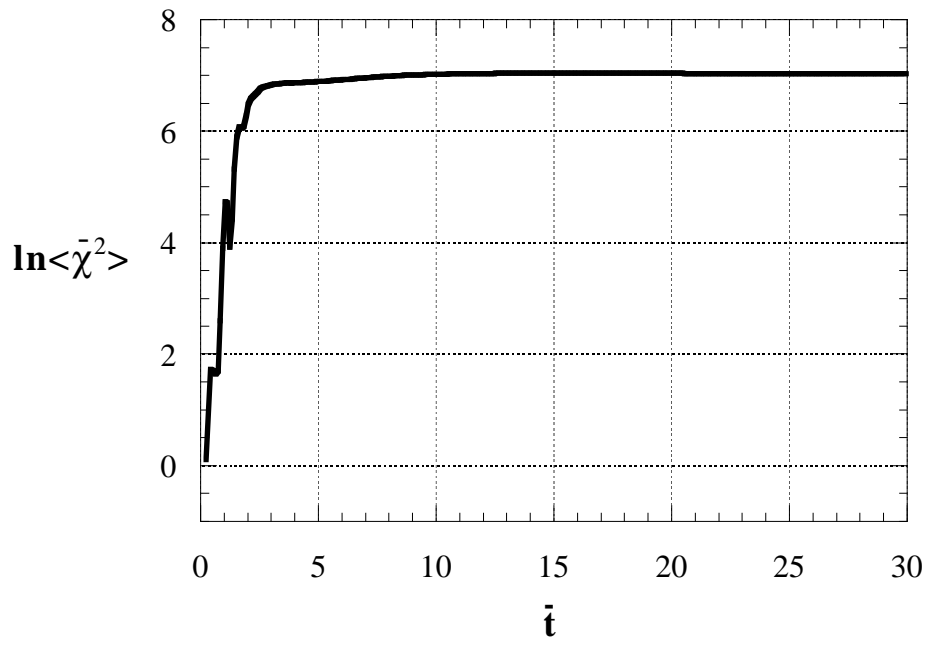
$g=0, \xi=200, m_\chi = m$



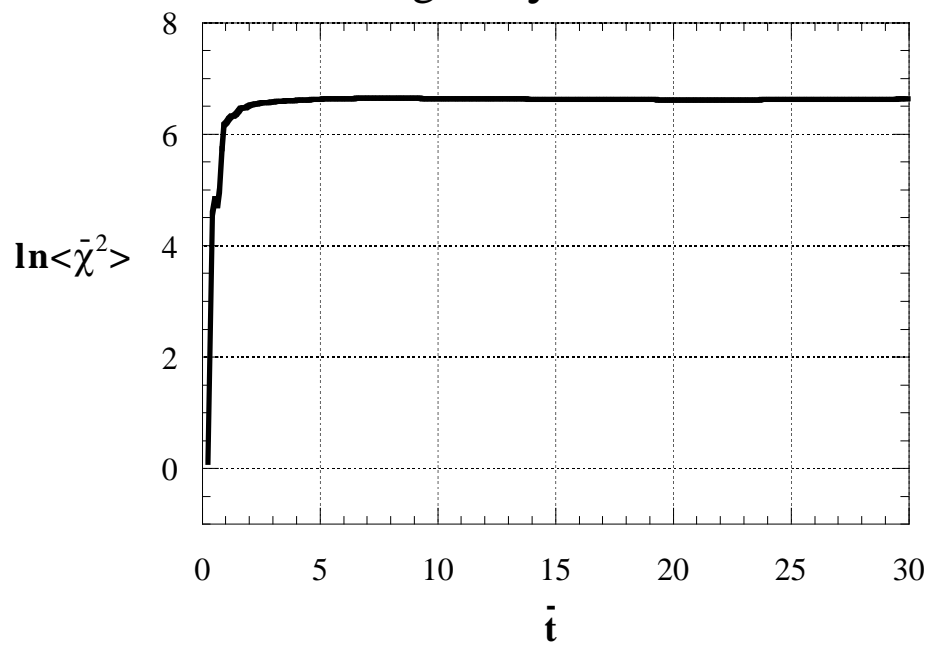
$g=0, \xi = -20$



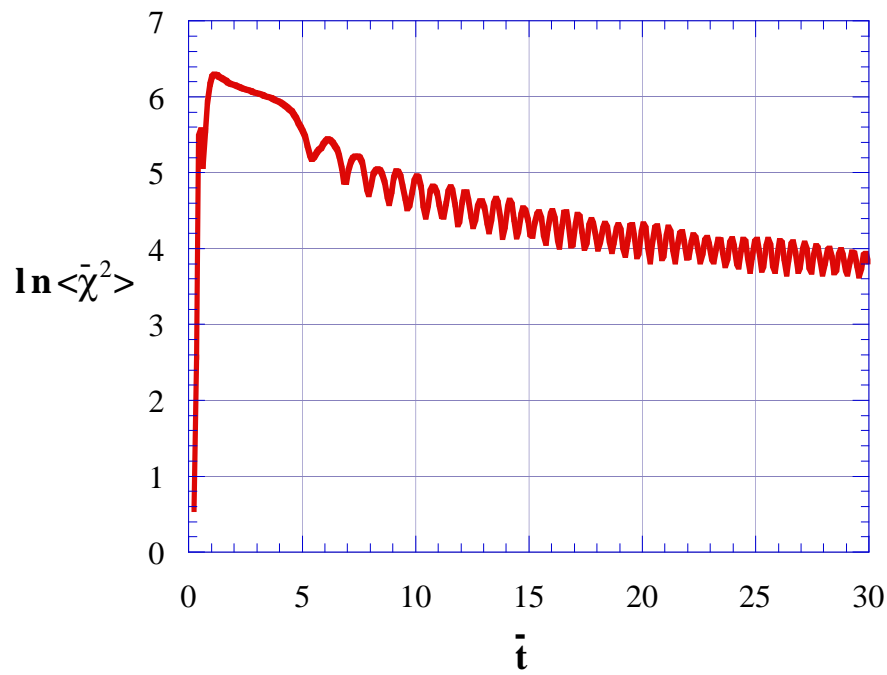
$g=0, \xi = -50$



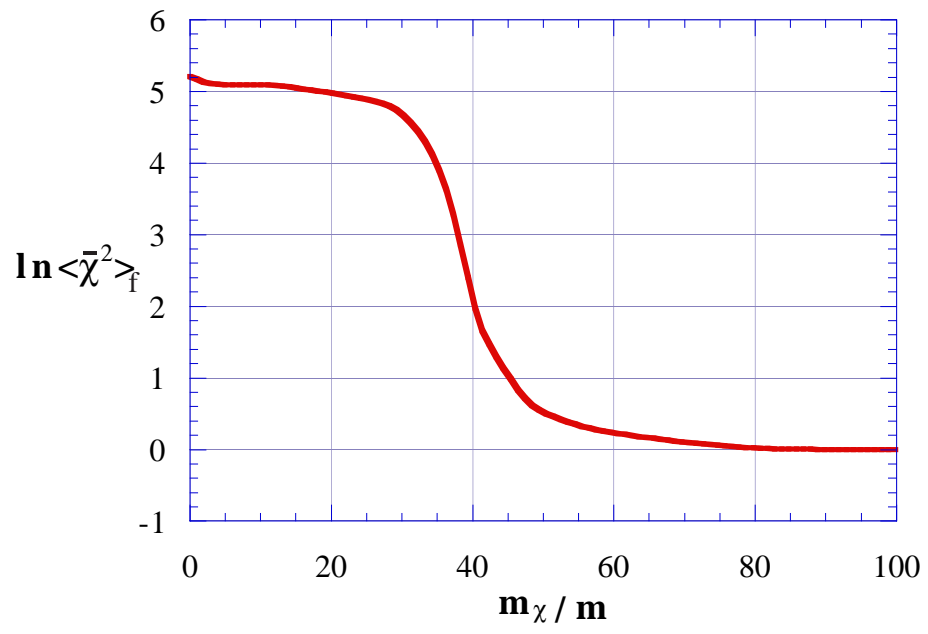
$g=0, \xi = -100$



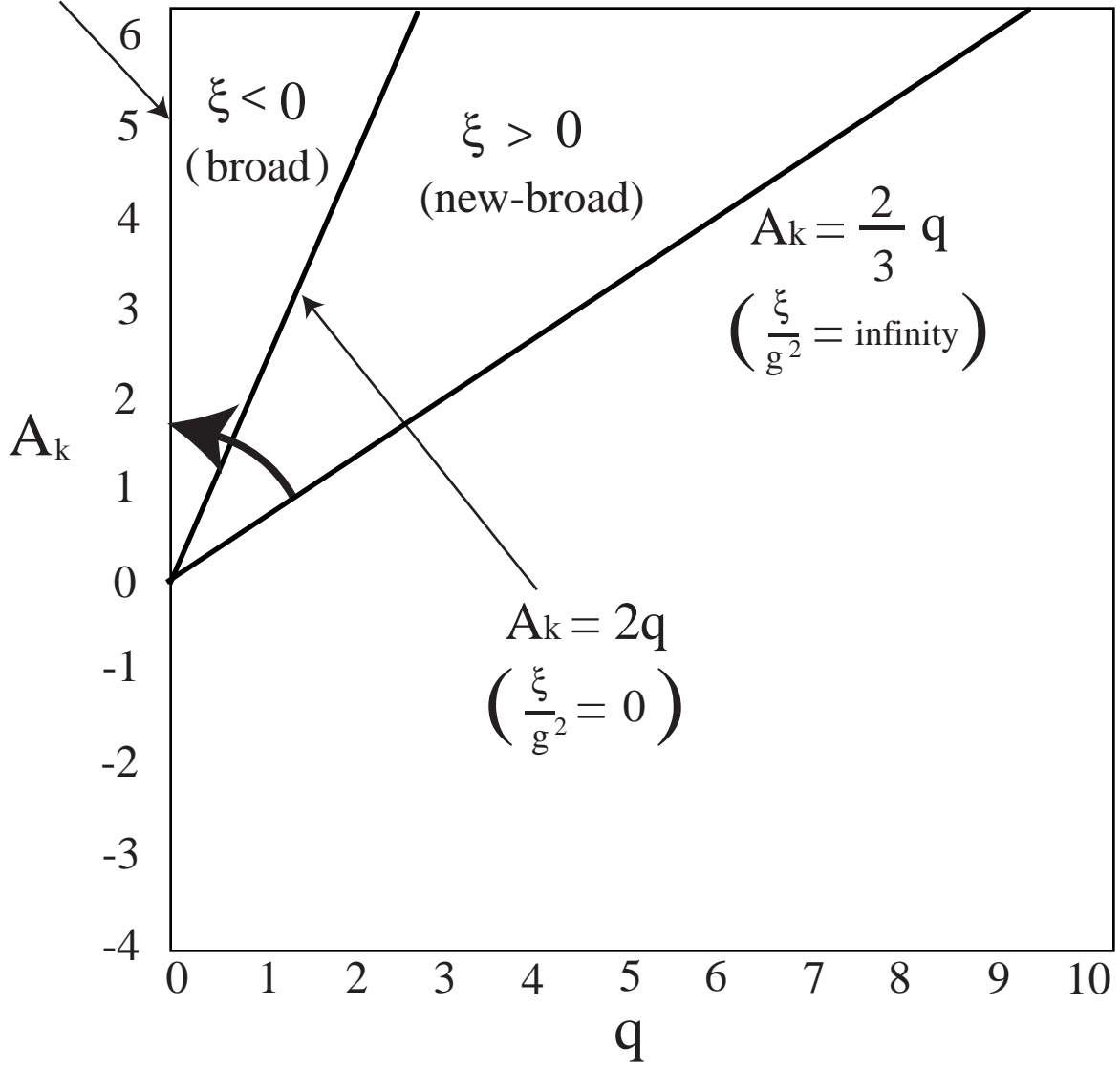
$g=0, \xi = -200, m_\chi = m$



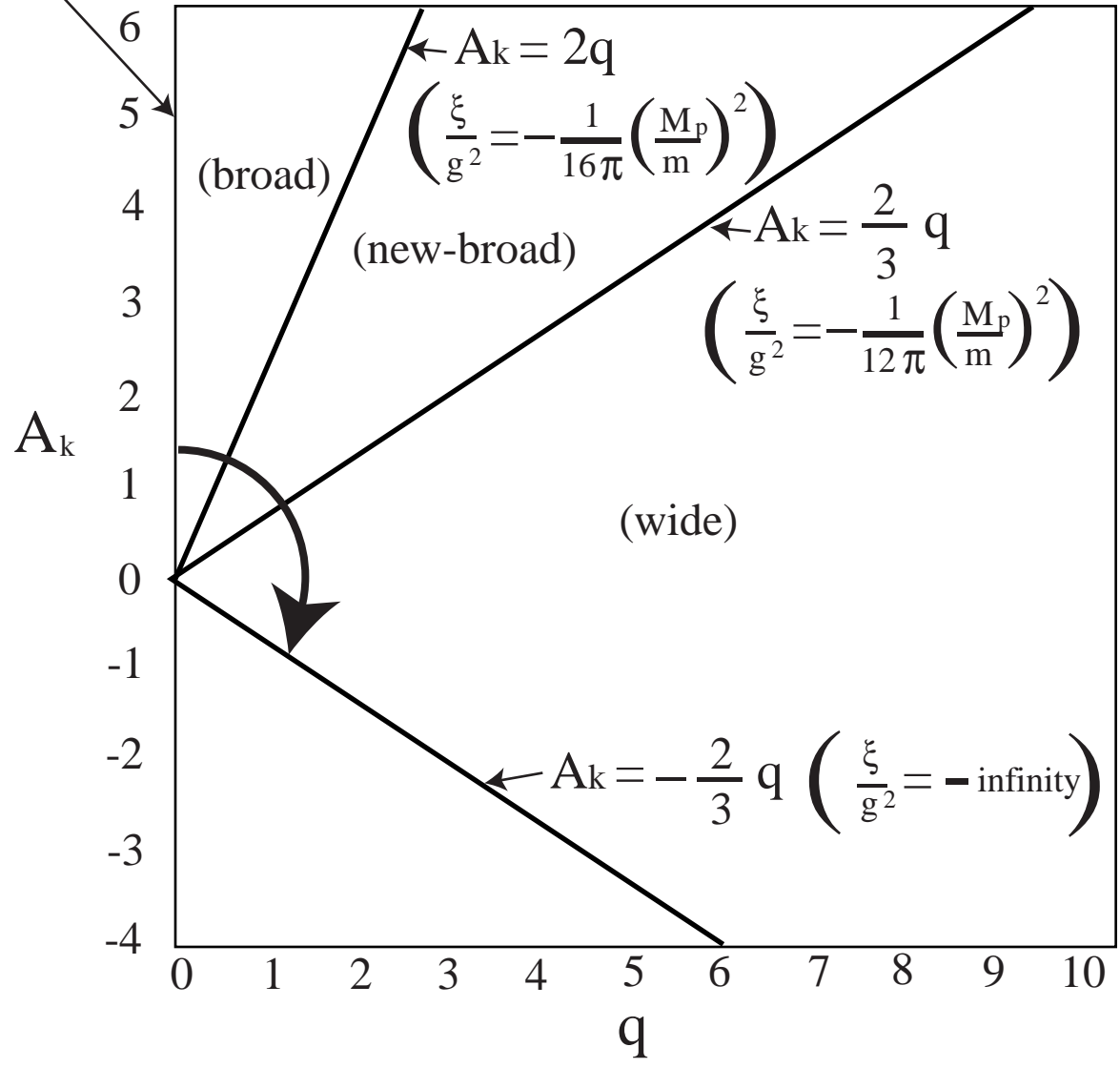
$\xi = -1000$ case



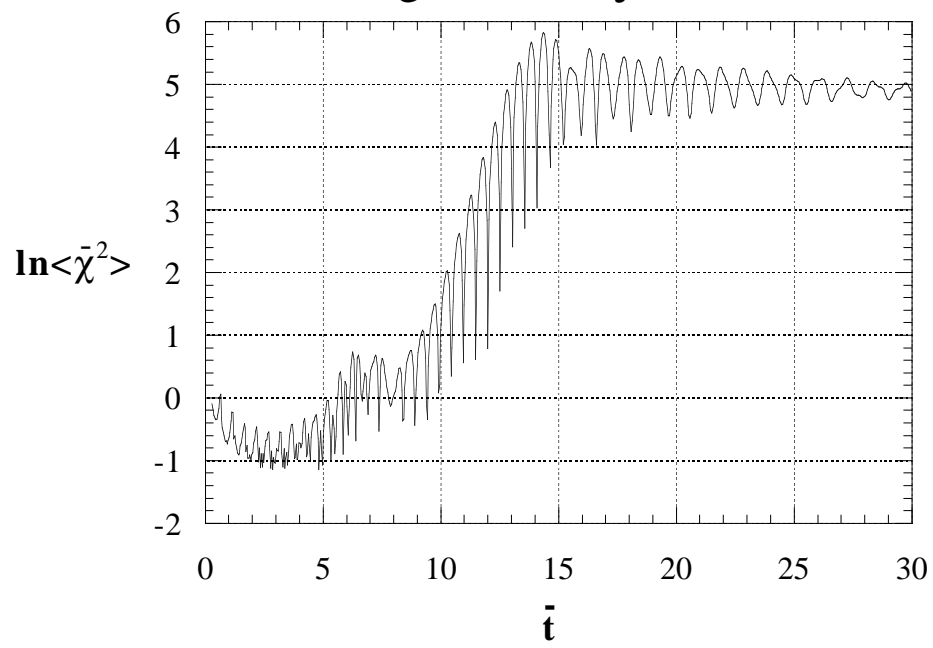
$$\frac{\xi}{g^2} = -\frac{1}{24\pi} \left(\frac{M_p}{m}\right)^2 \quad g^2 + 3\xi \kappa^2 m^2 > 0$$



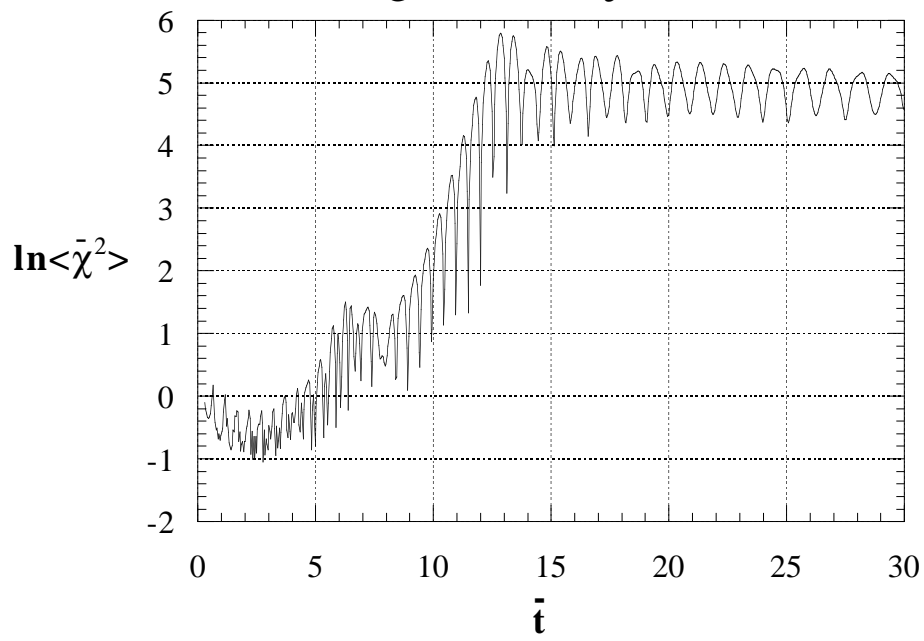
$$\frac{\xi}{g^2} = -\frac{1}{24\pi} \left(\frac{M_p}{m}\right)^2 \quad g^2 + 3\xi \kappa^2 m^2 < 0$$



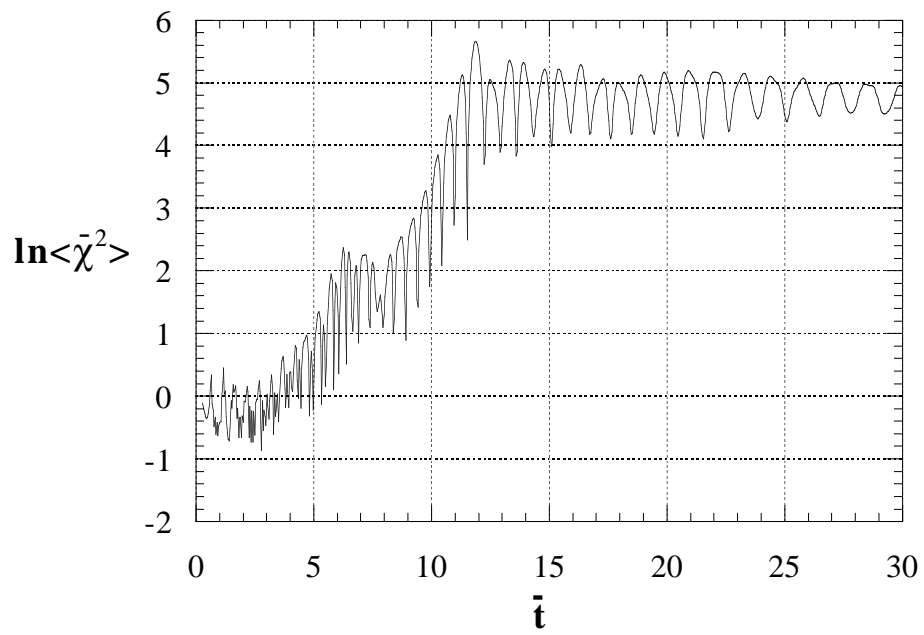
$g=3*10^{-4}, \xi=0$



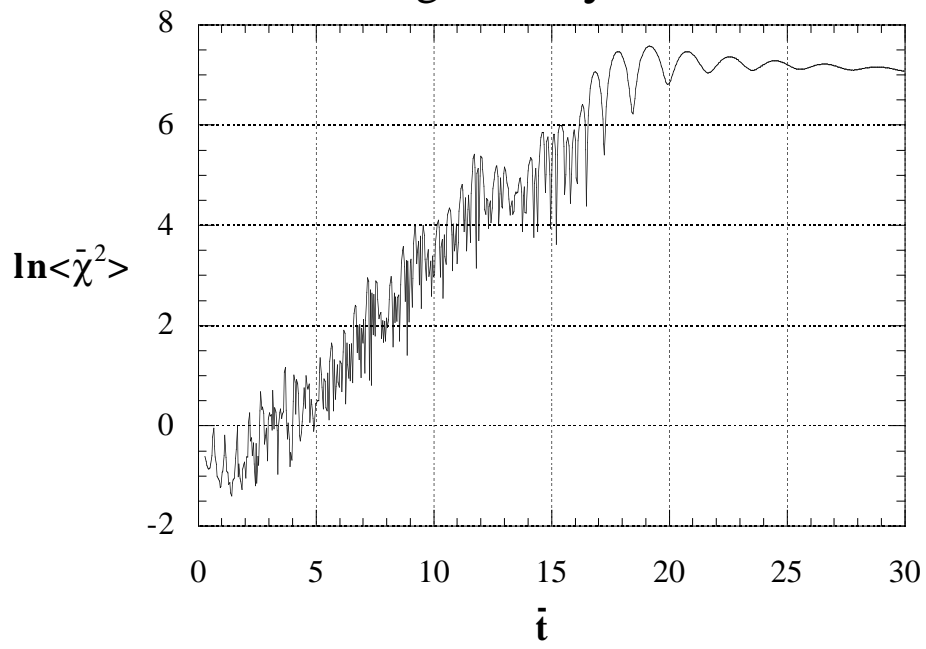
$g=3*10^{-4}, \xi = 50$



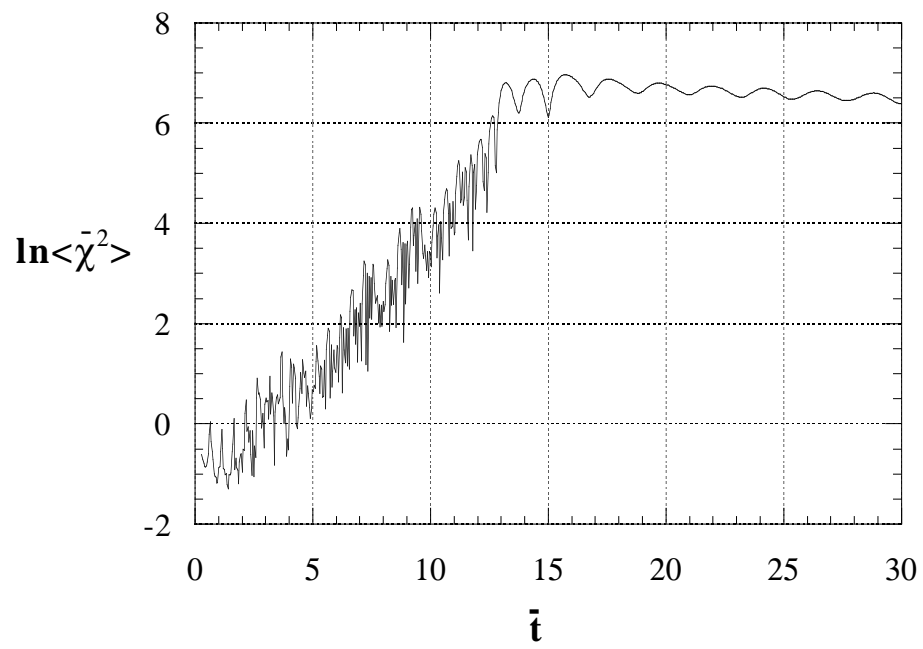
$g=3*10^{-4}, \xi =100$



$g=10^{-3}, \xi = 0$



$g=10^{-3}, \xi=50$



$g=10^{-3}, \xi=100$

